isvr Institute of Sound and Vibration Research

On Numerical Issues for the Wave/Finite Element Method

Y. Waki, B.R. Mace and M.J. Brennan

ISVR Technical Memorandum No 964

December 2006

University of Southampton

SCIENTIFIC PUBLICATIONS BY THE ISVR

Technical Reports are published to promote timely dissemination of research results by ISVR personnel. This medium permits more detailed presentation than is usually acceptable for scientific journals. Responsibility for both the content and any opinions expressed rests entirely with the author(s).

Technical Memoranda are produced to enable the early or preliminary release of information by ISVR personnel where such release is deemed to the appropriate. Information contained in these memoranda may be incomplete, or form part of a continuing programme; this should be borne in mind when using or quoting from these documents.

Contract Reports are produced to record the results of scientific work carried out for sponsors, under contract. The ISVR treats these reports as confidential to sponsors and does not make them available for general circulation. Individual sponsors may, however, authorize subsequent release of the material.

UNIVERSITY OF SOUTHAMPTON

INSTITUTE OF SOUND AND VIBRATION RESEARCH

DYNAMICS GROUP

On Numerical Issues for the Wave/Finite Element Method

by

Y. Waki, B.R. Mace and M.J. Brennan

ISVR Technical Memorandum No: 964

December 2006

Authorised for issue by
Professor M.J. Brennan
Group Chairman

TABLE OF CONTENTS

ABSTRACT

The waveguide finite element (WFE) method is a numerical method to investigate wave motion in a uniform waveguide. Numerical issues for the WFE method are specifically illustrated in this report. The method starts from finite element mass and stiffness matrices of only one element of the section of the waveguide. The matrices may be derived from commercial FE software such that existing element libraries can be used to model complex general structures. The transfer matrix, and hence the eigenvalue problem, is formed from the dynamic stiffness matrix in conjunction with a periodicity condition. The results of the eigenvalue problem represent the free wave characteristics in the waveguide. This report concerns numerical errors occurring in the WFE results and proposing approaches to improve the errors.

In the WFE method, numerical errors arise because of (1) the FE discretisation error, (2) round-off errors due to the inertia term and (3) ill-conditioning. The FE discretisation error becomes large when element length becomes large enough compared to the wavelength. However, the round-off error due to the inertia term becomes large for small element lengths when the dynamic stiffness matrix is formed. This tendency is illustrated by numerical examples for one-dimensional structures.

Ill-conditioning occurs when the eigenvalue problem is formed and solved and the resulting errors can become large, especially for complex structures. Zhong's method is used to improve the conditioning of the eigenvalue problem in this report. Errors in the eigenvalue problem are first mathematically discussed and Zhong's method validated. In addition, singular value decomposition is proposed to reduce errors in numerically determining the eigenvectors. For waveguides with a one-dimensional cross-section, the effect of the aspect ratio of the elements on the conditioning is also illustrated. For general structures, there is a crude trade-off between the conditioning, the FE discretisation error and the round-off error due to the inertia term. To alleviate the trade-off, the model with internal nodes is applied. At low frequencies, the approximate condensation formulation is derived and significant error reduction in the force eigenvector components is observed.

Three approaches to numerically calculate the group velocity are compared and the finite difference and the power and energy relationship are shown to be efficient approaches for general structures.

1. INTRODUCTION

1.1 Introduction

The waveguide finite element (WFE) method is a useful method when the dynamic behaviour of a uniform structure is of concern. The method involves the reformulation of the dynamic stiffness matrix, which includes the mass and stiffness matrices of a section of the structure, into the transfer matrix. Structural wave motion is expressed in terms of the eigenvalues and the eigenvectors of this matrix and these represent the wavenumbers and the wave modes respectively. However, several numerical difficulties arise when the problem is reformulated from a conventional finite element (FE) model. The aim of this report is (1) to identify and quantify the potential numerical problems and (2) to suggest alternative ways of determining the wave properties of a structure such that the numerical errors are reduced.

1.2 Overview of Periodic Structure Analysis

Many structures have uniformity or periodicity in certain directions. To analyse such structures, Floquet theory [1], which is one of the basic theories of wave propagation in periodic structures, or the transfer matrix method e.g. [2] can be used. The basic idea is that the propagation properties of waves in a periodic structure can be obtained from the propagation constants or by the transfer matrix. Although most of the early papers give the analytical dispersion relationship for relatively simple structures [3,4], numerical calculation is generally needed for complex structures. For complex structures, the finite element method (FEM) may be applied to calculate the propagation constants [5,6,7]. The transfer matrix is formed from the mass and stiffness matrices of discretised elements and the wave propagation characteristics are then described by the eigenvalues and eigenvectors of the transfer matrix.

The WFE method is based on this idea and several applications can be found in the literature. Early work can be found in [8] which investigated the propagation and stop band for periodic structures consisted from a beam and a plate. The forced response to random pressure fields was also presented. Thompson [9] and Gry et al [10,11] applied the method to analyse railway vibration, and Houillon et al [12] investigated wave motion in a general thin-shell structure. Duhamel et al [13] and Mace et al [14] discussed the accuracy of numerical

results for simple structures and Hinke et al [15] analysed wave properties in a sandwich panel. Mencik [16] formulated the problem of wave coupling between two general substructures and Maess [17] analysed a fluid filled pipe using an eigenpath analysis. One of the advantages of the WFE method is the computational cost [18] since this method needs information drawn from only one small section along the direction which the waves propagate. Another possible way of analysing such structures is the spectral finite element method [19] which uses a special shape function to represent the motion of a cross-section of the structure. However, this method needs special shape functions and element matrices to be developed for different wave types.

The WFE method needs only the conventional mass and stiffness matrices of a structure. Since the standard FE-package can be utilised to generate the stiffness and mass matrices, the full power of existing element libraries can be employed. In addition, since the wave characteristics are calculated for a given frequency, nearfield and oscillating decaying waves, which might be important for the system response near excitation points or discontinuities, can be effectively included. The forced response can be calculated using the wave approach (e.g. [20]).

1.3 Outline of the Report

The wave motion could be derived from the eigenvalues and eigenvectors of the transfer matrix. However, numerical difficulties may be encountered when solving the eigenvalue problem. Most papers mention the matrix conditioning of the eigenvalue problem [9,10,11,13,14,17] but do not discuss many details.

In this report, only free wave propagation is described and, in particular, numerical issues are discussed. First, the WFE formulation is briefly introduced and the conditioning of the eigenvalue problem is described. The application of the singular value decomposition (SVD) to determine the eigenvectors is proposed. Numerical errors in the eigenvalue problem are mathematically discussed and potential errors in the WFE method are enumerated. Numerical examples are presented for simple waveguides where the analytical solutions are available. The accuracy and validity of the results using different algorithms and FE models are also discussed. All calculations are performed in MATLAB. Finally some conclusions are drawn.

2. OVERVIEW OF THE WAVEGUIDE FINITE ELEMENT METHOD

2.1 Introduction

In this section, a brief overview of the WFE formulation is given. A small section of a structure is first modelled using FE. From the dynamic stiffness matrix of the elements the transfer matrix is formed. The transfer matrix describes the wave motion through the element and the eigenvalues and the eigenvectors of the resulting eigenvalue problem represent the wavenumbers and the wave modes in the structure.

2.2 Finite Element Formulation of a Structural Element

The equation of motion for uniform structural waveguides can be expressed as

$$\mathbf{M}\ddot{\mathbf{q}} + \mathbf{C}\dot{\mathbf{q}} + \mathbf{K}\mathbf{q} = \mathbf{f} \tag{2.1}$$

where **M**, **K**, and **C** are the mass, stiffness and damping matrices respectively, **f** represents the loading vector and **q** is the vector of the nodal displacement degrees of freedom (DOFs). Throughout this report, time harmonic motion $e^{j\omega t}$ is implicit. Equation (2.1) then becomes

$$\mathbf{D}\mathbf{q} = \left(-\omega^2\mathbf{M} + j\omega\mathbf{C} + \mathbf{K}\right)\mathbf{q} = \mathbf{f} \tag{2.2}$$

where **D** is the dynamic stiffness matrix. The nodal forces and DOFs are decomposed into sets associated with the left (L), right (R) cross-section and interior (I) nodes. For the case where there are no external forces on the interior nodes, equation (2.2) can be partitioned into

$$\begin{bmatrix} \mathbf{D}_{LL} & \mathbf{D}_{LR} & \mathbf{D}_{LI} \\ \mathbf{D}_{RL} & \mathbf{D}_{RR} & \mathbf{D}_{RI} \\ \mathbf{D}_{IL} & \mathbf{D}_{IR} & \mathbf{D}_{II} \end{bmatrix} \begin{bmatrix} \mathbf{q}_L \\ \mathbf{q}_R \\ \mathbf{q}_I \end{bmatrix} = \begin{bmatrix} \mathbf{f}_L \\ \mathbf{f}_R \\ \mathbf{0} \end{bmatrix} \tag{2.3}$$

which may be expressed as

$$\begin{bmatrix} \mathbf{D}_{MM} & \mathbf{D}_{MI} \\ \mathbf{D}_{IM} & \mathbf{D}_{II} \end{bmatrix} \begin{bmatrix} \mathbf{q}_M \\ \mathbf{q}_I \end{bmatrix} = \begin{bmatrix} \mathbf{f}_M \\ \mathbf{0} \end{bmatrix} \tag{2.4}$$

where the subscript M represents master nodes containing the left and right cross-section nodes. The second row of equation (2.4) leads to

$$\mathbf{q}_I = -\mathbf{D}_{II}^{-1}\mathbf{D}_{IM}\mathbf{q}_M \tag{2.5}$$

such that

$$\begin{bmatrix}\mathbf{q}_M \\ \mathbf{q}_I\end{bmatrix} = \begin{bmatrix}\mathbf{I} \\ -\mathbf{D}_{II}^{-1}\mathbf{D}_{IM}\end{bmatrix}\mathbf{q}_M = \mathbf{R}\mathbf{q}_M \tag{2.6}$$

where $\mathbf{I}$ is the identity matrix. Using the matrix $\mathbf{R}$ in equation (2.6), equation (2.4) becomes

$$\mathbf{R}^{\mathrm{T}}\begin{bmatrix}\mathbf{D}_{MM} & \mathbf{D}_{MI} \\ \mathbf{D}_{IM} & \mathbf{D}_{II}\end{bmatrix}\mathbf{R}\mathbf{q}_M = \mathbf{f}_M\,. \tag{2.7}$$

Expanding equation (2.7) leads to

$$\left[\mathbf{D}_{MM} - \mathbf{D}_{MI}\mathbf{D}_{II}^{-1}\mathbf{D}_{IM}\right]\mathbf{q}_M = \mathbf{f}_M \tag{2.8}$$

such that DOFs associated with internal nodes can be eliminated.

If the group velocity is calculated from the power flow and energy relationship stated later in this section, the form of equation (2.7) is useful to derive the reduced $\mathbf{M}, \mathbf{K}$ and $\mathbf{C}$ matrices. Putting these matrices instead of $\mathbf{D}$ into equation (2.7) readily gives the reduced matrices. The reduced mass matrix is, for example,

$$\mathbf{R}^{\mathrm{T}}\mathbf{M}\mathbf{R} = \mathbf{M}_{MM} - \mathbf{D}_{MI}\mathbf{D}_{II}^{-1}\mathbf{M}_{IM} - \mathbf{M}_{MI}\mathbf{D}_{II}^{-1}\mathbf{D}_{IM} + \mathbf{D}_{MI}\mathbf{D}_{II}^{-1}\mathbf{M}_{II}\mathbf{D}_{II}^{-1}\mathbf{D}_{IM}\,. \tag{2.9}$$

After removing internal DOFs, equation (2.2) for the section can be written as

$$\begin{bmatrix}\mathbf{D}_{LL} & \mathbf{D}_{LR} \\ \mathbf{D}_{RL} & \mathbf{D}_{RR}\end{bmatrix}\begin{bmatrix}\mathbf{q}_L \\ \mathbf{q}_R\end{bmatrix} = \begin{bmatrix}\mathbf{f}_L \\ \mathbf{f}_R\end{bmatrix}. \tag{2.10}$$

For a uniform section, the following relationships hold:

$$\mathbf{D}_{LL}^{\mathrm{T}} = \mathbf{D}_{LL},\ \mathbf{D}_{RR}^{\mathrm{T}} = \mathbf{D}_{RR},\ \mathbf{D}_{LR}^{\mathrm{T}} = \mathbf{D}_{RL} \tag{2.11}$$

and

$$\mathbf{D}_{RRij} = \mathrm{sgn}\cdot\mathbf{D}_{LLij}\ ,\quad \mathbf{D}_{RLij} = \mathrm{sgn}\cdot\mathbf{D}_{LRij} \tag{2.12}$$

where $\cdot^{\mathrm{T}}$ indicates the transpose and the signs in equations (2.12) depend on whether DOFs at the element interface are symmetric or anti-symmetric [9].

2.3 Wave Basis

Wave propagation can be described by the transfer matrix. The transfer matrix, hence the eigenvalue problem, can be formulated from the dynamic stiffness matrix. The eigenvalues and eigenvectors represent the wavenumbers and the wave mode shapes.

2.3.1 Transfer Matrix

The transfer matrix can be defined on the basis of the continuity of displacements and the equilibrium of forces of adjacent elements as [1]

$$\mathbf{T}\begin{bmatrix}\mathbf{q}_L\\ \mathbf{f}_L\end{bmatrix}=\begin{bmatrix}\mathbf{q}_R\\ -\mathbf{f}_R\end{bmatrix} \tag{2.13}$$

where $\mathbf{T}$ is the transfer matrix. The transfer matrix can be formed from the elements of the dynamic stiffness matrix as [13]

$$\mathbf{T}=\begin{bmatrix}-\mathbf{D}_{LR}^{-1}\mathbf{D}_{LL} & \mathbf{D}_{LR}^{-1}\\ -\mathbf{D}_{RL}+\mathbf{D}_{RR}\mathbf{D}_{LR}^{-1}\mathbf{D}_{LL} & -\mathbf{D}_{RR}\mathbf{D}_{LR}^{-1}\end{bmatrix}. \tag{2.14}$$

From a periodicity condition [1], free wave motion over the element length Δ is described in the form of an eigenvalue problem such that

$$\mathbf{T}\begin{bmatrix}\mathbf{q}\\ \mathbf{f}\end{bmatrix}=\lambda\begin{bmatrix}\mathbf{q}\\ \mathbf{f}\end{bmatrix}. \tag{2.15}$$

Although equation (2.15) formulates the basic principle for the WFE method, this eigenvalue problem is likely to be ill-conditioned for general problems because of the ill-conditioning of $\mathbf{D}_{LR}$ and the fact that the elements of the eigenvector range over a large magnitude. The conditioning of the eigenvalue problem is described in Section 3.

2.3.2 Eigenvalues and Eigenvectors

The eigenvalues λ_i in equation (2.15) relate to wave propagation over the distance Δ such that [1]

$$\lambda_i=e^{-jk_i\Delta} \tag{2.16}$$

where k_i represents the wavenumber for the ith wave. The wavenumber can be purely real, purely imaginary or complex, associated with a propagating, a nearfield (evanescent) or oscillating decaying wave respectively. The eigenvector corresponding to the ith eigenvalue can be expressed as

$$\mathbf{\Phi}_i=\begin{bmatrix}\mathbf{q}_i\\ \mathbf{f}_i\end{bmatrix}. \tag{2.17}$$

The eigenvector represents a wave mode and contains information about both the displacements and the internal forces. For uniform waveguides, there exist positive and negative going wave pairs in the form of $\lambda_i^{\pm}=e^{\pm jk_i\Delta}$ and the eigenvalues and associated

eigenvectors are expressed as $\left(\lambda_i, \boldsymbol{\Phi}_i^+\right)$ and $\left(1/\lambda_i, \boldsymbol{\Phi}_i^-\right)$. Positive-going waves are those for which the magnitude of the eigenvalues is less than 1, i.e. $|\lambda_i| < 1$ or if $|\lambda_i| = 1$, such that the power is positive going, i.e. $\mathrm{Re}\left\{\mathbf{f}^{\mathrm{H}}\dot{\mathbf{q}}\right\} = \mathrm{Im}\left\{\omega \mathbf{f}^{\mathrm{H}}\mathbf{q}\right\} > 0$ [13,14] where $\cdot^{\mathrm{H}}$ represents the complex conjugate transpose or Hermitian.

2.4 Group Velocity

The group velocity is the velocity at which the wave propagates. The group velocity for the *i*th wave is defined by (e.g. [21])

$$c_{gi} = \frac{\partial \omega}{\partial k_i}. \tag{2.18}$$

There are several approaches to the numerical calculation of the group velocity.

The finite difference method calculates the group velocity from a first order approximation as

$$c_{gi}^{(n)} = \frac{\omega^{(n+1)} - \omega^{(n-1)}}{k_i^{(n+1)} - k_i^{(n-1)}} \tag{2.19}$$

where n-1, n, n+1 are consecutive discrete frequencies. Other definitions for equation (2.19) are possible. Once the dispersion relationship is determined, the group velocity can be obtained.

Another approach for the group velocity is in terms of the power and energy as [21]

$$c_{gi} = \frac{P_i}{E_{tot,i}} \tag{2.20}$$

where P is the time average power transmission thorough the cross section of a waveguide and E_{tot} is the total energy density. These values are given by [14,21]

$$P_i = \frac{1}{2}\mathrm{Re}\left\{\mathbf{f}_i^{\mathrm{H}}\dot{\mathbf{q}}_i\right\} = \frac{\omega}{2}\mathrm{Im}\left\{\mathbf{f}_i^{\mathrm{H}}\mathbf{q}_i\right\}. \tag{2.21}$$

and

$$\begin{aligned} &E_{tot,i} = E_{k,i} + E_{p,i}, \\ &E_{k,i} = \frac{1}{4\Delta}\mathrm{Re}\left\{\dot{\mathbf{q}}_i^{\mathrm{H}}\mathbf{M}\dot{\mathbf{q}}_i\right\} = -\frac{\omega^2}{4\Delta}\mathrm{Re}\left\{\mathbf{q}_i^{\mathrm{H}}\mathbf{M}\mathbf{q}_i\right\},\ E_{p,i} = \frac{1}{4\Delta}\mathrm{Re}\left\{\mathbf{q}_i^{\mathrm{H}}\mathbf{K}\mathbf{q}_i\right\} \end{aligned} \tag{2.22}$$

where $E_{k,i}$ and $E_{p,i}$ represent the kinetic and potential energy densities for the *i*th wave. The dissipated power follows from the imaginary part of **K** and/or the damping matrix **C**.

In addition, the group velocity could be determined directly by differentiating the eigenproblem [22]. The group velocity can be expressed as

$$c_{gi} = \frac{\partial \omega}{\partial k_i} = \frac{1}{2\omega}\frac{\partial \omega^2}{\partial k_i} \tag{2.23}$$

and $\partial k / \partial \omega^2$ is found from the differentiation of the eigenvalue problem (2.15) such that

$$\frac{\partial}{\partial\left(\omega^2\right)}\left\{\left(\mathbf{T}-\lambda\mathbf{I}\right)\mathbf{\Phi}_i\right\} = \mathbf{0}\,. \tag{2.24}$$

Expanding equation (2.24), using equations (2.16), (2.23) and premultiplying by the left eigenvector $\mathbf{\Psi}_i$ leads to

$$\mathbf{\Psi}_i\left(\frac{\partial}{\partial\left(\omega^2\right)}\mathbf{T} + \frac{j\Delta}{2\omega}\lambda_i\frac{\partial k_i}{\partial \omega}\mathbf{I}\right)\mathbf{\Phi}_i = 0\,. \tag{2.25}$$

Recalling equation (2.14), noting the differentiation of the matrix inverse [23], $\frac{\partial}{\partial\left(\omega^2\right)}\mathbf{D}_{LR}^{-1} = -\mathbf{D}_{LR}^{-1}\mathbf{M}_{LR}\mathbf{D}_{LR}^{-1}$, $\partial\mathbf{T}/\partial\left(\omega^2\right)$ in equation (2.25) can be evaluated as

$$\frac{\partial}{\partial\left(\omega^2\right)}\mathbf{T} = \begin{bmatrix} -\mathbf{D}_{LR}^{-1}\mathbf{M}_{LR}\mathbf{D}_{LR}^{-1}\mathbf{D}_{LL} + \mathbf{D}_{LR}^{-1}\mathbf{M}_{LL} & \mathbf{D}_{LR}^{-1}\mathbf{M}_{LR}\mathbf{D}_{LR}^{-1} \\ \mathbf{M}_{RL} - \mathbf{M}_{RR}\mathbf{D}_{LR}^{-1}\mathbf{D}_{LL} + & \\ \mathbf{D}_{RR}\mathbf{D}_{LR}^{-1}\mathbf{M}_{LR}\mathbf{D}_{LR}^{-1}\mathbf{D}_{LL} - \mathbf{D}_{RR}\mathbf{D}_{LR}^{-1}\mathbf{M}_{LL} & \mathbf{M}_{RR}\mathbf{D}_{LR}^{-1} - \mathbf{D}_{RR}\mathbf{D}_{LR}^{-1}\mathbf{M}_{LR}\mathbf{D}_{LR}^{-1} \end{bmatrix}. \tag{2.26}$$

From the above equations the group velocity is given by

$$c_{gi} = -\frac{j\Delta\lambda_i}{2\omega}\frac{\mathbf{\Psi}_i\mathbf{I}\mathbf{\Phi}_i}{\mathbf{\Psi}_i\dfrac{\partial}{\partial\left(\omega^2\right)}\mathbf{T}\mathbf{\Phi}_i}\,. \tag{2.27}$$

Three formulations of the group velocity have been introduced. The accuracy of each approach is discussed later in this report.

3. NUMERICAL ISSUES AND IMPLEMENTATION

3.1 Introduction

In this section, the conditioning of the eigenvalue problem is illustrated. Numerical errors occurring in the eigenvalue problem are mathematically explained and the conditioned eigenvalue problem is introduced. In particular, the singular value decomposition (SVD) is applied to reduce errors for numerically determining the eigenvectors. Numerical errors in the WFE method are then enumerated.

3.2 Conditioning of the Eigenvalue Problem

The eigenvalue problem was formulated using the transfer matrix (2.15). However, the results from the eigenvalue problem might be inaccurate. In this section the conditioned eigenvalue problem is introduced and SVD application is proposed to reduce numerical inaccuracies for determining the eigenvectors.

3.2.1 Mathematical Background of Numerical Errors in the Eigenvalue Problem

Numerical errors occur (1) when the eigenvalue problem is formulated and (2) when the eigenvalue problem is solved. When the eigenvalue problem (2.14) is formulated, numerical errors can arise predominantly from the matrix inversion. The maximum resulting errors for the matrix inversion $\mathbf{A}^{-1}$ can be of the order of $\varepsilon \cdot \kappa(\mathbf{A})$ where ε is the machine precision and

$$\kappa(\mathbf{A}) = \|\mathbf{A}\|\|\mathbf{A}^{-1}\| = \sigma_{\max}/\sigma_{\min} \tag{3.1}$$

is the condition number [24], $\|\cdot\|$ is the 2-norm and, $\sigma_{\max}$ and $\sigma_{\min}$ are the largest and smallest singular values. For general matrices, the matrix can be ill-conditioned if there are comparatively large numbers on the off-diagonal elements, e.g.[24,25]. When the transfer

matrix approach (2.15) is formed, $\mathbf{D}_{LR}^{-1}$ should be calculated which in general might be ill-conditioned. This causes numerical errors when the eigenvalue problem is formed.

Next, numerical errors occurring in the solution of the eigenproblem are discussed. The matrix for the eigenvalue problem in the WFE method is square, complex and non-symmetric. For such matrix Schur factorisation is known to be most useful in numerical analysis because all matrices, including defective ones, can be factored in this way [24]. Major software packages such as MATLAB and Mathematica use Schur factorisation for solving such eigenvalue problems.

Many different approaches for assessing the error bounds on the computed eigenvalues and eigenvectors have been proposed, e.g. [26,27]. A well-known estimate for the error bound is given by Gerschgorin's theorem [24]. However, this theorem usually gives a large error bound for an ill-conditioned matrix. More precisely, the following discussion holds for Schur factorisation [25].

When the eigenvalue problem $\mathbf{A}\boldsymbol{\Phi} = \lambda\boldsymbol{\Phi}$ or $\boldsymbol{\Psi}^{\mathrm{H}}\mathbf{A} = \lambda\boldsymbol{\Psi}^{\mathrm{H}}$ is solved using Schur factorisation, the matrix $\mathbf{A}$ is factorised into the form $\mathbf{Q}^{\mathrm{H}}\mathbf{A}\mathbf{Q} = \mathbf{D} + \mathbf{N}$ where $\mathbf{Q}$ is unitary, $\mathbf{D}$ is diagonal and $\mathbf{N}$ is strictly upper-triangular [25]. The resulting errors for the eigenvalue problem are estimated from $\kappa(\mathbf{Q})$ or $\|\mathbf{N}\|$ [25]. If $\kappa(\mathbf{Q})$ is large then the eigenvector matrix is ill-conditioned. If the eigenvectors are far from orthogonal to each other, the results may contain large errors [24,25]. Since the eigenvectors in the transfer matrix approach (2.15) contains both the displacement and force components and usually each eigenvector is far from orthogonal to each other, $\kappa(\mathbf{Q})$ is likely to be issue for general cases. A large value for $\|\mathbf{N}\|$ means that $\mathbf{A}$ is far from normal, e.g. strongly asymmetric [25]. Such eigenvalue problems are likely to have a large error in the computed results, which is the case for the transfer matrix approach stated in equation (2.14).

Specifically, for $n \geq 5$ for the $n \times n$ matrix $\mathbf{A}$, there is no analytical expression for the roots of the characteristic polynomial so that the eigensolver must be iterative [24]. For a matrix of large size, conditioning becomes more important for errors when Schur factorisation is applied to solve the eigenvalue problem. In this report, the matrix size for a rod and a beam is $n = 2, 4$ respectively such that conditioning effects are small. However, the conditioning becomes important for a plate example as the matrix size becomes large.

It is worth noting that if the eigenvalue problem is ill-conditioned, complex conjugate eigenvalues occur as numerical artefacts [25] if

$$\frac{\|\mathbf{E}\|}{\|\mathbf{A}\|} \le \frac{1}{\sqrt{s(\lambda_i)^2 - 1}} \tag{3.2}$$

where $\mathbf{E}$ is the perturbation matrix incurred from the round-off error because of the finite digit arithmetic and $s(\lambda_i)$ is the sensitivity of the eigenvalue with respect to the perturbation, given by [25]

$$s(\lambda_i) = 1 \Big/ \left| \boldsymbol{\Psi}(\lambda_i)^{\mathrm{H}} \boldsymbol{\Phi}(\lambda_i) \right| \quad (\ge 1) \tag{3.3}$$

with $\|\boldsymbol{\Phi}_i\| = \|\boldsymbol{\Psi}_i\| = 1$. Under the condition (3.2), two distinct but similar eigenvalues λ_i, λ_j become repeated eigenvalues λ_i', λ_j' whose values are different from both λ_i and λ_j [25]. Examples using MATLAB eigenvalue solvers can be found in [28,29].

3.2.2 Overview of the Conditioning for the Eigenvalue Problem

To improve the ill-conditioned problem (2.15), several works [10,13,14,15,16] applied Zhong's algorithm [30]. The details can be seen in [30,31,32]. This method formulates the conditioned, general eigenvalue problem such that $\mathbf{D}_{LR}$ is not necessarily inverted. In addition, since the eigenvector contains only displacement components, numerical error could be reduced because $\kappa(\mathbf{Q})$ can be smaller. Thompson [9] also derived the similar eigenvalue problem using symmetric relationships, e.g. equations (2.11), (2.12), which results in smaller size of the eigenvalue problem.

In this report, Zhong's algorithm has been applied because the approach seems well matched with the problems which have been considered so far.

3.2.3 Zhong's Method and Practical Implementation

Zhong's method [30] is illustrated in this section. The method starts from a reformulation of equation (2.13) into the relationships for the displacement vectors alone:

$$\begin{bmatrix} \mathbf{q}_L \\ \mathbf{f}_L \end{bmatrix} = \begin{bmatrix} \mathbf{I}_n & \mathbf{0} \\ \mathbf{D}_{LL} & \mathbf{D}_{LR} \end{bmatrix} \begin{bmatrix} \mathbf{q}_L \\ \mathbf{q}_R \end{bmatrix}, \quad \begin{bmatrix} \mathbf{q}_R \\ \mathbf{f}_R \end{bmatrix} = \begin{bmatrix} \mathbf{0} & \mathbf{I}_n \\ -\mathbf{D}_{RL} & -\mathbf{D}_{RR} \end{bmatrix} \begin{bmatrix} \mathbf{q}_L \\ \mathbf{q}_R \end{bmatrix}. \tag{3.4}$$

After some matrix operations using the periodicity condition and the symplectic relationship [30], equations (3.4) can be rearranged as

$$\begin{bmatrix} -\mathbf{D}_{RL} & -\mathbf{D}_{LL} - \mathbf{D}_{RR} \\ \mathbf{0} & -\mathbf{D}_{RL} \end{bmatrix} \begin{bmatrix} \mathbf{q}_L \\ \lambda \mathbf{q}_L \end{bmatrix} = \lambda \begin{bmatrix} \mathbf{0} & \mathbf{D}_{LR} \\ -\mathbf{D}_{RL} & \mathbf{0} \end{bmatrix} \begin{bmatrix} \mathbf{q}_L \\ \lambda \mathbf{q}_L \end{bmatrix}, \tag{3.5}$$

and

$$\begin{bmatrix} \mathbf{D}_{LR} & \mathbf{0} \\ \mathbf{D}_{RR}+\mathbf{D}_{LL} & \mathbf{D}_{LR} \end{bmatrix}\begin{bmatrix} \mathbf{q}_L \\ \lambda\mathbf{q}_L \end{bmatrix} = \frac{1}{\lambda}\begin{bmatrix} \mathbf{0} & \mathbf{D}_{LR} \\ -\mathbf{D}_{RL} & \mathbf{0} \end{bmatrix}\begin{bmatrix} \mathbf{q}_L \\ \lambda\mathbf{q}_L \end{bmatrix}. \tag{3.6}$$

Adding equations (3.5) and (3.6) gives the general eigenvalue problem:

$$\mu\mathbf{Z}_1\begin{bmatrix} \mathbf{q} \\ \lambda\mathbf{q} \end{bmatrix} = \mathbf{Z}_2\begin{bmatrix} \mathbf{q} \\ \lambda\mathbf{q} \end{bmatrix} \tag{3.7}$$

with

$$\mathbf{Z}_1 = \begin{bmatrix} \mathbf{0} & \mathbf{D}_{LR} \\ -\mathbf{D}_{RL} & \mathbf{0} \end{bmatrix},\quad \mathbf{Z}_2 = \begin{bmatrix} \left(\mathbf{D}_{LR}-\mathbf{D}_{RL}\right) & -\left(\mathbf{D}_{LL}+\mathbf{D}_{RR}\right) \\ \left(\mathbf{D}_{LL}+\mathbf{D}_{RR}\right) & \left(\mathbf{D}_{LR}-\mathbf{D}_{RL}\right) \end{bmatrix} \tag{3.8}$$

where $\mu = \lambda + 1/\lambda$ and the subscript L for the eigenvector is suppressed for clarity. For symmetric elements, several elements of $\mathbf{Z}_2$ in equation (3.7) cancel each other as certain relationships (2.11), (2.12) hold and $\mathbf{Z}_1$ and $\mathbf{Z}_2$ in equation (3.7) become skew-symmetric.

In practice, it is recommended that either $\mathbf{Z}_1$ or $\mathbf{Z}_2$ is inverted such that the standard eigenvalue problem

$$\mu\begin{bmatrix} \mathbf{q} \\ \lambda\mathbf{q} \end{bmatrix} = \mathbf{Z}_1^{-1}\mathbf{Z}_2\begin{bmatrix} \mathbf{q} \\ \lambda\mathbf{q} \end{bmatrix} \text{ or } \frac{1}{\mu}\begin{bmatrix} \mathbf{q} \\ \lambda\mathbf{q} \end{bmatrix} = \mathbf{Z}_2^{-1}\mathbf{Z}_1\begin{bmatrix} \mathbf{q} \\ \lambda\mathbf{q} \end{bmatrix} \tag{3.9}$$

is formulated. To reduce numerical errors, the matrix with the smaller condition number should be inverted [33]. In addition, the pseudo matrix inverse (e.g. [24]) can be applied to reduce numerical errors.

One might be interested in only several waves with small wavenumbers. A limiting case is when a wave is at the cut-off frequency (usually $k \to 0$) such that usually $\mu = \lambda + 1/\lambda \to 2$. In such cases, it is beneficial to take the form of $\mu - 2$ $\left(\text{or } 1/\mu - 0.5\right)$ rather than μ $\left(1/\mu\right)$ in equations (3.9) such that the important eigenvalues can be bounded by several smallest (largest) values.

Equations (3.9) are a standard, double eigenvalue problem whose eigenvectors contain only the displacement components. The original eigenvalues $\lambda_i, 1/\lambda_i$ can be determined from the calculated eigenvalue $\mu_i = \lambda_i + 1/\lambda_i$ by solving the quadratic equation or by using a trigonometric function of the form $\mu_i = \lambda_i + 1/\lambda_i = e^{-jk_i\Delta} + e^{jk_i\Delta} = 2\cos\left(k_i\Delta\right)$.

There are two independent eigenvectors $\boldsymbol{\varphi}_1, \boldsymbol{\varphi}_2$ associated with the double eigenvalues, which are given by

$$\boldsymbol{\varphi}_{1,2} = \begin{bmatrix} \mathbf{q}_{1,2} \\ \lambda \mathbf{q}_{1,2} \end{bmatrix}. \tag{3.10}$$

The original eigenvector associated with eigenvalues $\lambda_i, 1/\lambda_i$ can be found from a linear combination of $\boldsymbol{\varphi}_1, \boldsymbol{\varphi}_2$ [13,14,30], i.e.,

$$\boldsymbol{\varphi} = \begin{bmatrix} \mathbf{q} \\ \lambda \mathbf{q} \end{bmatrix} = \alpha_1 \boldsymbol{\varphi}_1 + \alpha_2 \boldsymbol{\varphi}_2 \ . \tag{3.11}$$

Substituting equations (3.11) and (3.10) into equation (3.5) gives

$$\begin{bmatrix} -\mathbf{D}_{RL} & -\mathbf{D}_{LL} - \mathbf{D}_{RR} - \lambda \mathbf{D}_{LR} \\ \lambda \mathbf{D}_{RL} & -\mathbf{D}_{RL} \end{bmatrix} \left\{ \alpha_1 \begin{bmatrix} \mathbf{q}_1 \\ \lambda \mathbf{q}_1 \end{bmatrix} + \alpha_2 \begin{bmatrix} \mathbf{q}_2 \\ \lambda \mathbf{q}_2 \end{bmatrix} \right\} = \mathbf{0}. \tag{3.12}$$

Taking the scalar product of $\boldsymbol{\varphi}_1^{\mathrm{H}}$ leads to the relationship between α_1 and α_2 such that [13]

$$\frac{\alpha_2}{\alpha_1} = -\frac{\begin{bmatrix} \mathbf{q}_1^{\mathrm{H}} & \lambda \mathbf{q}_1^{\mathrm{H}} \end{bmatrix} \begin{bmatrix} -\mathbf{D}_{RL} & -\mathbf{D}_{LL} - \mathbf{D}_{RR} - \lambda \mathbf{D}_{LR} \\ \lambda \mathbf{D}_{RL} & -\mathbf{D}_{RL} \end{bmatrix} \begin{bmatrix} \mathbf{q}_1 \\ \lambda \mathbf{q}_1 \end{bmatrix}}{\begin{bmatrix} \mathbf{q}_1^{\mathrm{H}} & \lambda \mathbf{q}_1^{\mathrm{H}} \end{bmatrix} \begin{bmatrix} -\mathbf{D}_{RL} & -\mathbf{D}_{LL} - \mathbf{D}_{RR} - \lambda \mathbf{D}_{LR} \\ \lambda \mathbf{D}_{RL} & -\mathbf{D}_{RL} \end{bmatrix} \begin{bmatrix} \mathbf{q}_2 \\ \lambda \mathbf{q}_2 \end{bmatrix}}. \tag{3.13}$$

Although equation (3.13) is algebraically correct, there may be some difficulties when calculating it numerically. In the next section, an alternative way of determining the eigenvectors is investigated using singular value decomposition (SVD).

3.2.4 Application of SVD for Determination of Eigenvectors

The eigenvectors could be obtained from equation (3.13) but numerical problems may occur. For the limiting case $\lambda \to 1$, equation (3.13) approaches $\alpha_2/\alpha_1 \to 0/0$ and round-off errors during arithmetic calculations become large.

Alternatively, SVD may be applied. Equation (3.12) can be written in another form as

$$\begin{bmatrix} -\mathbf{D}_{RL} & -\mathbf{D}_{LL} - \mathbf{D}_{RR} - \lambda \mathbf{D}_{LR} \\ \lambda \mathbf{D}_{RL} & -\mathbf{D}_{RL} \end{bmatrix} \begin{bmatrix} \mathbf{q}_1 & \mathbf{q}_2 \\ \lambda \mathbf{q}_1 & \lambda \mathbf{q}_2 \end{bmatrix} \begin{bmatrix} \alpha_1 \\ \alpha_2 \end{bmatrix} = \mathbf{0}. \tag{3.14}$$

Writing equation (3.14) as $\mathbf{A}\begin{bmatrix} \alpha_1 & \alpha_2 \end{bmatrix}^{\mathrm{T}} = \mathbf{0}$ with an $n \times 2$ rectangular matrix **A**, where *n* is the length of the eigenvector, the problem is now to solve an overdetermined simultaneous equation if $n \geq 3$. SVD can be applied to solve an overdetermined linear equation [34]. Performing SVD on **A** gives

$$\mathbf{A} = \mathbf{U}\mathbf{S}\mathbf{V}^{H} \tag{3.15}$$

where the matrix dimensions are $\mathbf{A}\in\mathbb{C}(n\times 2), \mathbf{U}\in\mathbb{C}(n\times n), \mathbf{S}\in\mathbb{R}(n\times 2), \mathbf{V}\in\mathbb{C}(2\times 2)$. Equation (3.15) can be written as

$$\mathbf{A}\begin{bmatrix} v_{11} & v_{12} \\ v_{21} & v_{22} \end{bmatrix} = \mathbf{U}\begin{bmatrix} \sigma_1 & 0 & 0 & \cdots & 0 \\ 0 & \sigma_\varepsilon(\approx 0) & 0 & \cdots & 0 \end{bmatrix}^{\mathrm{T}}. \tag{3.16}$$

The matrix **S** contains two singular values on its leading diagonal and one of these is almost zero. The second column of equation (3.16) and expanding **A** to the original expression gives

$$\begin{bmatrix} -\mathbf{D}_{RL} & -\mathbf{D}_{LL}-\mathbf{D}_{RR}-\lambda\mathbf{D}_{LR} \\ \lambda\mathbf{D}_{RL} & -\mathbf{D}_{RL} \end{bmatrix}\begin{bmatrix} \mathbf{q}_1 & \mathbf{q}_2 \\ \lambda\mathbf{q}_1 & \lambda\mathbf{q}_2 \end{bmatrix}\begin{bmatrix} v_{12} \\ v_{22} \end{bmatrix} \approx \mathbf{0} \tag{3.17}$$

such that $\begin{bmatrix}\alpha_1 & \alpha_2\end{bmatrix}^{\mathrm{T}}$ are given by

$$\frac{\alpha_2}{\alpha_1} = \frac{v_{22}}{v_{21}}. \tag{3.18}$$

The advantages of SVD approach are

(1) equation (3.18) can be derived from only one matrix multiplication while equation (3.13) needs two multiplications for both the denominator and numerator such that numerical errors through the matrix operations can be reduced and,

(2) the orders of v_{21}, v_{22} in equation (3.18) are typically $O(1)$ while that of the original values α_1, α_2 in equation (3.13) may be very small.

After finding the vector of displacements from equations (3.11) and (3.18), the corresponding force eigenvector can be calculated from the first row of equation (2.15) as

$$\mathbf{f} = (\mathbf{D}_{LL} + \lambda\mathbf{D}_{LR})\mathbf{q}. \tag{3.19}$$

The original right eigenvector associated with λ_i is then

$$\mathbf{\Phi}_i = \mathbf{\Phi}(\lambda_i) = \begin{bmatrix} \mathbf{q}(\lambda_i) \\ \mathbf{f}(\lambda_i) \end{bmatrix} = \begin{bmatrix} \mathbf{q}(\lambda_i) \\ (\mathbf{D}_{LL} + \lambda_i\mathbf{D}_{LR})\mathbf{q}(\lambda_i) \end{bmatrix}. \tag{3.20}$$

Similarly, the original left eigenvector can be obtained as [13]

$$\mathbf{\Psi}_i = \mathbf{\Psi}(\lambda_i) = \begin{bmatrix} \mathbf{q}(1/\lambda_i)^{\mathrm{T}}(\mathbf{D}_{RR} + \lambda_i\mathbf{D}_{LR}) & \mathbf{q}(1/\lambda_i)^{\mathrm{T}} \end{bmatrix}. \tag{3.21}$$

3.3 Numerical Errors in the WFE Method

Even if the conditioned eigenvalue problem is solved, numerical errors still occur. Errors arising in the WFE method are enumerated and each is explained.

3.3.1 Errors in the Conditioned Eigenvalue Problem

The sequential procedure for the WFE method, based on the conditioned eigenvalue problem, can be illustrated as follows. The damping matrix **C** is excluded for simplicity.

(1) Discretise a section of a structure of length Δ using FE such that **K**, **M** are formed.

(2) Calculate the dynamic stiffness matrix $\mathbf{D} = \mathbf{K} - \omega^2\mathbf{M}$ for each frequency.

(3) Formulate the standard eigenvalue problem, i.e. equation (3.9).

(4) Solve the eigenvalue problem.

(5) Calculate the original eigenvalues and eigenvectors, i.e. equations (3.11) and (3.18).

(6) Calculate the force components from equation (3.20).

For steps (3)-(5), the conditioning is essential to reduce numerical errors for a matrix of large size. For step (1), the FE discretisation error should be first considered and specifically for step (2), the round-off error can be important. Each error is explained.

3.3.2 FE Discretisation Error

When a structure is discretised using FE, FE discretisation errors occur. To represent the system motion accurately, 6 or more FE are generally needed for each wavelength [35]. In the WFE formula, this criterion can be expressed as [13]

$$k\Delta \le 1. \tag{3.22}$$

Equation (3.22) should be satisfied both along the waveguide and over its cross-section.

For accurate results, small Δ is needed for large wavenumbers. However, very small Δ is inappropriate because the conditioning is likely to deteriorate and the round-off error due to the inertia term increases. The section length Δ should be carefully determined when the structure is modelled. Examples will be shown in Sections 4 and 5.

3.3.2 Round-Off Errors in the Dynamic Stiffness Matrix

The round-off errors occur in every numerical arithmetic operation. Specifically, this error can be important when the dynamic stiffness matrix, $\mathbf{D} = \mathbf{K} - \omega^2\mathbf{M}$, is numerically calculated. The error becomes large when $\left|\mathbf{K}_{ij}\right| \gg \left|\omega^2\mathbf{M}_{ij}\right|$ because of the finite precisions of arithmetic operations.

It should be noted that the criteria where the round-off errors become large depends not only on ω but also the length Δ. Small Δ increases $\left|\mathbf{K}_{ij}\right|$ but decreases $\left|\mathbf{M}_{ij}\right|$ for the discretised elements. When significant effective digit numbers of the inertia term are rounded,

D becomes inaccurate such that the eigenvalue problem cannot be accurately formed. To evaluate the round-off error due to the inertia term, $\min\left(\left|\omega^2\mathbf{M}_{ii}\right|/\left|\mathbf{K}_{ii}\right|\right)$ may be a indication since some off-diagonal terms may not be important. To reduce this error, Δ should not be too small when the structure is modelled.

To solve the compromise between the FE discretisation error and the round-off error due to the inertia, condensation using internal nodes can be used. If a structure is modelled with internal nodes and DOFs associated with the internal nodes are reduced using equation (2.7), the round-off error could be reduced. A numerical example is shown in Section 5.

4. NUMERICAL EXAMPLES OF A ROD AND A BEAM

4.1 Introduction

The quasi-longitudinal waves in a rod and flexural waves in a beam are considered. The accuracy of results calculated by the WFE method is discussed in this section. No damping is assumed.

4.2 Quasi-Longitudinal Waves in a Rod

The quasi-longitudinal waves in a rod are considered in this section. The WFE results are compared with the analytical solution and the accuracies are evaluated.

4.2.1 Discretisation of a Rod Element

The mass and stiffness matrices for the rod element can be modelled using a linear shape function such that [35]

$$\mathbf{K} = \frac{EA}{\Delta}\begin{bmatrix} 1 & -1 \\ -1 & 1 \end{bmatrix}, \quad \mathbf{M} = \frac{\rho A \Delta}{6}\begin{bmatrix} 2 & 1 \\ 1 & 2 \end{bmatrix} \tag{4.1}$$

where E is the Young's modulus, A is the cross-sectional area, ρ is the mass density and Δ is the length of a section. The dynamic stiffness matrix, $\mathbf{D} = \mathbf{K} - \omega^2\mathbf{M}$, then becomes

$$\mathbf{D} = \frac{EA}{\Delta}\begin{bmatrix} 1-\frac{(k_L\Delta)^2}{3} & -1-\frac{(k_L\Delta)^2}{6} \\ sym. & 1-\frac{(k_L\Delta)^2}{3} \end{bmatrix} \tag{4.2}$$

where

$$k_L = \sqrt{\rho/E}\,\omega \tag{4.3}$$

is the quasi-longitudinal wavenumber [36]. The dynamic stiffness matrix in equation (4.2) is accurate for the analytical dynamic stiffness matrix [37] up to $O\left\{(k_L\Delta)^2\right\}$ with error being

$O\left\{\left(k_L\Delta\right)^4\right\}$ for small $k_L\Delta$. The transfer matrix (2.14) can be obtained from equation (4.2) [13] such that

$$\mathbf{T}=\frac{1}{1+\dfrac{\left(k_L\Delta\right)^2}{6}}\begin{bmatrix} 1-\dfrac{\left(k_L\Delta\right)^2}{3} & -\dfrac{\Delta}{EA} \\ \dfrac{EA}{\Delta}\left\{\left(k_L\Delta\right)^2-\dfrac{\left(k_L\Delta\right)^4}{12}\right\} & 1-\dfrac{\left(k_L\Delta\right)^2}{3} \end{bmatrix}. \tag{4.4}$$

4.2.2 Analytical Expressions for the Eigenvalues and Eigenvectors

The analytical solution for the WFE formulation can be found from equation (4.4). The eigenvalues are analytically given as [13]

$$\lambda^{\pm}=\frac{1}{1+\dfrac{\left(k_L\Delta\right)^2}{6}}\left\{1-\frac{\left(k_L\Delta\right)^2}{3}\mp j\left(k_L\Delta\right)\sqrt{1-\frac{\left(k_L\Delta\right)^2}{12}}\right\}. \tag{4.5}$$

For small $k_L\Delta$, equation (4.5)can be expanded to

$$\lambda^{\pm}=1\mp jk_L\Delta-\frac{\left(k_L\Delta\right)^2}{2}\pm j\frac{5\left(k_L\Delta\right)^3}{24}+\cdots \tag{4.6}$$

and this is accurate up to $O\left\{\left(k_L\Delta\right)^2\right\}$ with error being $O\left\{\left(k_L\Delta\right)^3\right\}$. It should be noted that the error in the wavenumber given from $\log\left(\lambda^{\pm}\right)/-j=k^{\pm}\Delta$ becomes from equation (4.6)

$$\left(k\Delta\right)^{\pm}=\pm k_L\Delta\left(1+\frac{\left(k_L\Delta\right)^2}{8}\mp\cdots\right) \tag{4.7}$$

such that relative error in the wavenumber is $O\left\{\left(k_L\Delta\right)^2\right\}$.

The right eigenvectors associated with the eigenvalues (4.5) can be analytically obtained as

$$\mathbf{\Phi}^{\pm}=\begin{bmatrix}u\\ f\end{bmatrix}=\begin{bmatrix}1\\ \mp jEAk\sqrt{1-\dfrac{\left(k_L\Delta\right)^2}{12}}\end{bmatrix} \tag{4.8}$$

where u is the longitudinal displacement and f is the normal force. The exact solution for a continuous rod is [36]

$$\left[f/u\right]^{\pm}=\mp jEAk\,. \tag{4.9}$$

The force eigenvector per unit displacement in equation (4.8) can be simplified to

$$\left[f/u\right]_{WFE}^{\pm} = \mp jEAk\left\{1-\left(k_L\Delta\right)^2/24\right\} \tag{4.10}$$

for small $k_L\Delta$ with the relative error being $O\left\{\left(k_L\Delta\right)^2\right\}$.

4.2.3 Relative Errors in the Eigenvalues and Eigenvectors

Figures 4.1, 4.2 show the relative errors in the wavenumber, $\left(k-k_L\right)/k_L$, and the force eigenvector per unit displacement, $\left(f_{WFE}-f\right)/f$, respectively. In both figures, the trend of the curve is same. The relative errors increase for $k_L\Delta > 3\cdot 10^{-4}$ because of the FE discretisation error and, for $k_L\Delta < 3\cdot 10^{-4}$ because of the round-off errors due to the inertia term. Although the size of the error is small for very small $k_L\Delta$, it should be noted that not only the magnitude but also the phase of the force eigenvector fluctuates such that the forced response of the system will fluctuate because of the numerical errors. When the forced response at low frequencies is of concern, length of the element Δ should be chosen as enough large to reduce the round-off errors due to the inertia term.

Asymptotic slopes in the relative errors at large $k_L\Delta$ and small $k_L\Delta$ are +20 dB/decade and -20 dB/decade, respectively. For large $k_L\Delta$, the asymptotic slope is about +20 dB/decade in both figures. This behaviour can be explained from equations (4.7) for the wavenumber (Figure 4.1) and equation (4.10) for the eigenvector (Figure 4.2).

For small $k_L\Delta$, the round-off error is dominant for the relative errors such that the minimum value of $\left|\omega^2\mathbf{M}_{ii}\right|/\left|\mathbf{K}_{ii}\right|$ is of concern since some off-diagonal terms may not be important for general cases. From equations (4.1), it is given that $\min\left(\left|\omega^2\mathbf{M}_{ii}\right|/\left|\mathbf{K}_{ii}\right|\right) = 1/3\left(k_L\Delta\right)^2$. From this estimation, the round-off error due to the inertia term is related to $\left(k_L\Delta\right)^{-2}$, which is same as the asymptotic slope in the relative errors. If the ratio is greater than 10^{16} $\left(k_L\Delta < 10^{-8}\right)$, all the inertia terms could be rounded in double precision calculation as can be seen in the figures.

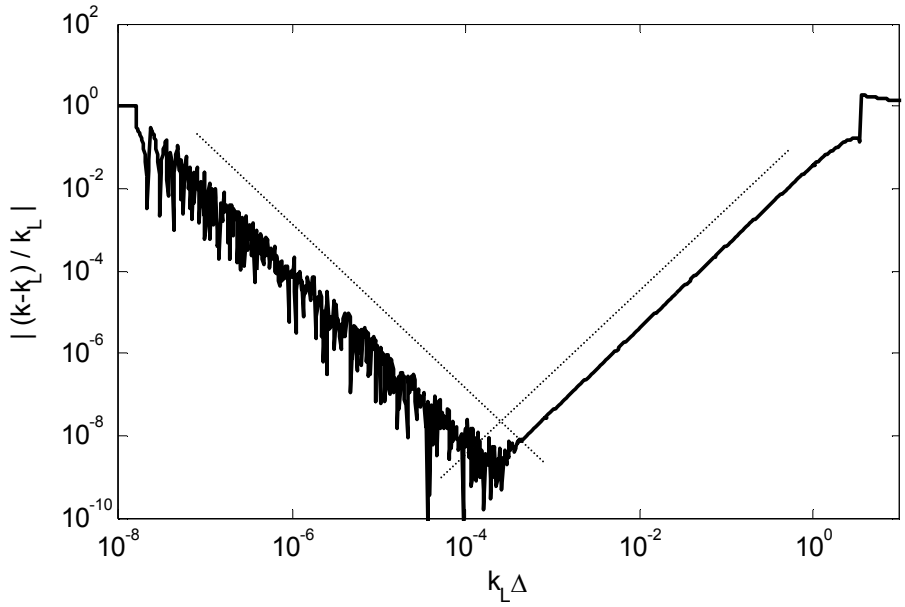

Figure 4.1: Relative error in the wavenumber: ····· asymptote $\pm 20dB/decade$.

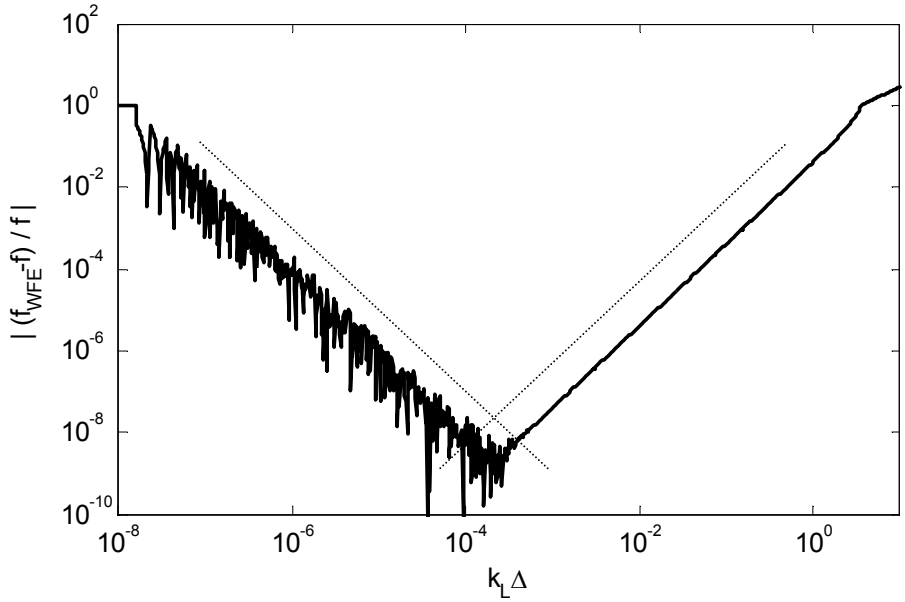

Figure 4.2: Relative error in the eigenvector: ····· asymptote $\pm 20dB/decade$.

4.2.4 Relative Errors in the Group Velocity

The group velocity is numerically calculated using the approaches illustrated in Section 2.4. The relative errors in the group velocity $\left(c_{g(WFE)} - c_g\right)/c_g$ are plotted in Figure 4.3 where c_g is the analytical group velocity, $c_g = \sqrt{E/\rho}$ [21]. The analysed frequency range is linearly discretised into 1000 frequency steps in the log scale.

For all methods, the relative error is almost same above $k_L\Delta > 10^{-3}$. The relative error of the power and energy relationship is smallest below $k_L\Delta < 10^{-3}$. Since the group velocity is calculated from the power flow and the energy density given in equations (2.21) and (2.22), small fluctuated errors in the eigenvectors can be improved through the calculation. At this frequency range, the relative error for the differentiation of the eigenproblem shows the almost same curve as those in the wavenumber and eigenvector while that the error for the finite difference method is larger very slightly. Although the error for the finite difference method depends on the frequency step, too small frequency step does not always improve the error because the error becomes more sensitive to the errors in the dispersion relationship.

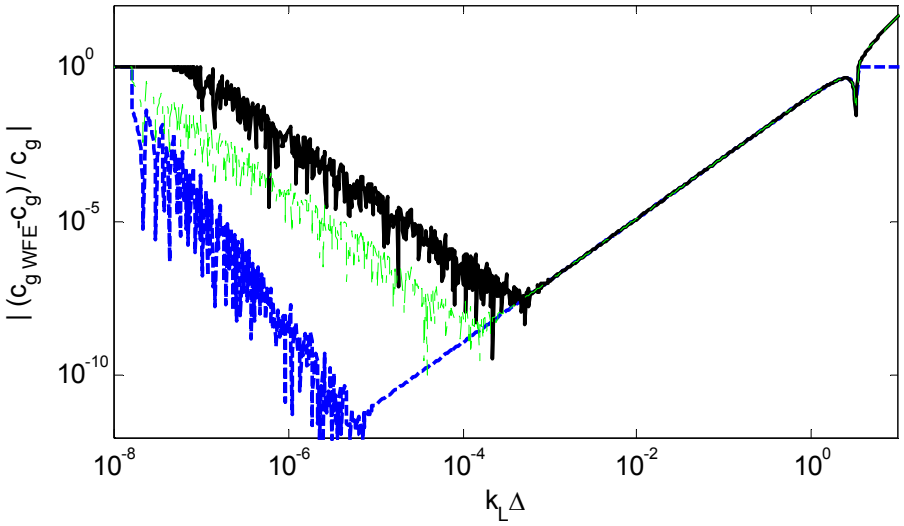

Figure 4.3: Relative errors in the group velocity: — finite difference, – – power and energy relationship, –·– differentiation of the eigenproblem.

4.3 Flexural Waves in an Euler-Bernoulli Beam

The flexural waves in the Euler-Bernoulli beam (e.g. [36]) are considered. The WFE results are evaluated with the analytical solution.

4.3.1 Analytical Expression for the Discretised Beam Element

Using a cubic polynomial as a shape function, the mass and stiffness matrices of the beam can be formulated as [35]

$$\mathbf{K}=\frac{EI}{\Delta^3}\begin{bmatrix} 12 & 6\Delta & -12 & 6\Delta \\ & 4\Delta^2 & -6\Delta & 2\Delta^2 \\ sym. & & 12 & -6\Delta \\ & & & 4\Delta^2 \end{bmatrix},\ \mathbf{M}=\frac{\rho A\Delta}{420}\begin{bmatrix} 156 & 22\Delta & 54 & -13\Delta \\ & 4\Delta^2 & 13\Delta & -3\Delta^2 \\ sym. & & 156 & -22\Delta \\ & & & 4\Delta^2 \end{bmatrix} \tag{4.11}$$

where EI is the bending stiffness, ρ is the mass density and A is the cross-sectional area. The dynamic stiffness matrix then becomes

$$\mathbf{D}=\frac{EI}{\Delta^3}\begin{bmatrix} \left(12-\frac{156}{420}(k_B\Delta)^4\right) & \Delta\left(6-\frac{22}{420}(k_B\Delta)^4\right) & \left(-12-\frac{54}{420}(k_B\Delta)^4\right) & \Delta\left(6+\frac{13}{420}(k_B\Delta)^4\right) \\ & \Delta^2\left(4-\frac{4}{420}(k_B\Delta)^4\right) & \Delta\left(-6-\frac{13}{420}(k_B\Delta)^4\right) & \Delta^2\left(2+\frac{3}{420}(k_B\Delta)^4\right) \\ sym. & & \left(12-\frac{156}{420}(k_B\Delta)^4\right) & \Delta\left(-6+\frac{22}{420}(k_B\Delta)^4\right) \\ & & & \Delta^2\left(4-\frac{4}{420}(k_B\Delta)^4\right) \end{bmatrix} \tag{4.12}$$

where

$$k_B=\sqrt[4]{\frac{\rho A}{EI}}\sqrt{\omega} \tag{4.13}$$

is the bending wavenumber [36]. The dynamic stiffness matrix in equation (4.2) is accurate for the analytical dynamic stiffness matrix [37] up to $O\left\{(k_B\Delta)^4\right\}$ with error being $O\left\{(k_B\Delta)^8\right\}$ for small $k_B\Delta$.

The transfer matrix derived from equation (4.12) becomes [13]

$$\mathbf{T}=\frac{1}{302400+720\left(k_B\Delta\right)^4+\left(k_B\Delta\right)^8}\times$$

$$\begin{bmatrix} 302400+13320\left(k_B\Delta\right)^4+26\left(k_B\Delta\right)^8 & \Delta\left(302400+3240\left(k_B\Delta\right)^4+2\left(k_B\Delta\right)^8\right) \\ \dfrac{50400\left(k_B\Delta\right)^4+120\left(k_B\Delta\right)^8}{\Delta} & 302400+13320\left(k_B\Delta\right)^4+10\left(k_B\Delta\right)^8 \\ \dfrac{EI\left(302400\left(k_B\Delta\right)^4+2820\left(k_B\Delta\right)^8+\frac{7}{2}\left(k_B\Delta\right)^{12}\right)}{\Delta^3} & \dfrac{EI\left(151200\left(k_B\Delta\right)^4+570\left(k_B\Delta\right)^8+\frac{1}{4}\left(k_B\Delta\right)^{12}\right)}{\Delta^2} \\ \dfrac{EI\left(-151200\left(k_B\Delta\right)^4-570\left(k_B\Delta\right)^8-\frac{1}{4}\left(k_B\Delta\right)^{12}\right)}{\Delta^2} & \dfrac{EI\left(-50400\left(k_B\Delta\right)^4-78\left(k_B\Delta\right)^8-\frac{1}{60}\left(k_B\Delta\right)^{12}\right)}{\Delta} \end{bmatrix}$$

$$\begin{bmatrix} \dfrac{\Delta^3\left(50400+180\left(k_B\Delta\right)^4\right)}{EI} & \dfrac{\Delta^2\left(-151200-780\left(k_B\Delta\right)^4\right)}{EI} \\ \dfrac{\Delta^2\left(151200+780\left(k_B\Delta\right)^4\right)}{EI} & \dfrac{\Delta\left(-302400-3240\left(k_B\Delta\right)^4\right)}{EI} \\ 302400+13320\left(k_B\Delta\right)^4+26\left(k_B\Delta\right)^8 & \dfrac{-50400\left(k_B\Delta\right)^4-120\left(k_B\Delta\right)^8}{\Delta} \\ \Delta\left(-302400-3240\left(k_B\Delta\right)^4-2\left(k_B\Delta\right)^8\right) & 302400+13320\left(k_B\Delta\right)^4+10\left(k_B\Delta\right)^8 \end{bmatrix} \quad .(4.14)$$

Approximate solutions for the characteristic equation derived from the transfer matrix (4.14) are [13]

$$\begin{aligned} \lambda_{1,2}\left(k_B\Delta\right)&=1\mp j\left(k_B\Delta\right)-\frac{1}{2}\left(k_B\Delta\right)^2\pm\frac{j}{6}\left(k_B\Delta\right)^3+\frac{1}{24}\left(k_B\Delta\right)^4\mp\frac{23j}{2880}\left(k_B\Delta\right)^5-\cdots, \\ \lambda_{3,4}\left(k_B\Delta\right)&=1\mp\left(k_B\Delta\right)+\frac{1}{2}\left(k_B\Delta\right)^2\mp\frac{1}{6}\left(k_B\Delta\right)^3+\frac{1}{24}\left(k_B\Delta\right)^4\mp\frac{23}{2880}\left(k_B\Delta\right)^5-\cdots \end{aligned} \quad (4.15)$$

where $\lambda_{1,2}$ are related to the propagating waves and $\lambda_{3,4}$ to the nearfield waves. From equations (4.15) the eigenvalues are accurate up to $O\left\{\left(k_B\Delta\right)^4\right\}$ with error being $O\left\{\left(k_B\Delta\right)^5\right\}$. The relative errors in the wavenumber, $\log\left(\lambda\right)/-j=k\Delta$, are from equation (4.15)

$$\begin{aligned} \left(k_B\Delta\right)_{1,2}&=\left(k_B\Delta\right)\left\{\pm1\mp\frac{577}{2880}\left(k_B\Delta\right)^4+\cdots\right\}, \\ \left(k_B\Delta\right)_{3,4}&=-j\left(k_B\Delta\right)\left\{\pm1\mp\frac{577}{2880}\left(k_B\Delta\right)^4+\cdots\right\} \end{aligned} \quad (4.16)$$

such that the relative error in the wavenumbers are $O\left\{\left(k_B\Delta\right)^4\right\}$.

The eigenvectors associated with $\lambda_{1,2}$ are also analytically given such that

$$\begin{bmatrix} w_{12} \\ \theta_{12}\Delta \\ f_{12}\Delta^3/EI \\ m_{12}\Delta^2/EI \end{bmatrix} = \begin{bmatrix} 1 \\ \mp j(k_B\Delta)\left\{1 \mp (k_B\Delta)^4/2880 \pm (k_B\Delta)^6/10800 \mp \cdots\right\} \\ \pm j(k_B\Delta)^3\left\{1 \mp (k_B\Delta)^4/960 \mp 13(k_B\Delta)^6/302400 \pm \cdots\right\} \\ -(k_B\Delta)^2\left\{1 - (k_B\Delta)^4/1440 - (k_B\Delta)^6/18900 - \cdots\right\} \end{bmatrix} \tag{4.17}$$

where w is the translational displacement and θ, f, m are the rotational displacement, the shear force and the moment per unit displacement. The analytical solution is available anywhere (e.g. [20,36]). The relative error in the elements of the analytical eigenvectors (4.17) are $O\left\{(k_B\Delta)^4\right\}$. Similar expression holds for $\lambda_{3,4}$ with the relative error in the elements of the eigenvectors being $O\left\{(k_B\Delta)^4\right\}$.

Although the details are omitted, the same accuracies are given using the conditioned eigenvalue problem (3.9), i.e. the relative error is $O\left\{(k_B\Delta)^4\right\}$ for the wavenumbers and components in the eigenvectors.

4.3.2 Relative Errors in the Eigenvalues and Eigenvectors

The relative errors in the wavenumbers (eigenvalues) and eigenvectors are investigated in this section. The properties of the beam are assumed to be $EI = 0.175$, $\rho A = 0.078$ and Δ is selected as $2 \cdot 10^{-3}$, all in SI units. The results using both the transfer matrix approach (2.15) and the conditioned eigenvalue problem (3.9) are compared.

Figure 4.4 shows the relative errors in the propagating wavenumber using both eigenvalue problems. Regardless of the eigenvalue problems, the relative errors take the minimum around $k_B\Delta = 0.04$ and the similar trend with the quasi-longitudinal waves can be seen. That is, the FE discretisation errors govern the relative errors for large $k_B\Delta$ while for the round-off errors due to the inertia term become significant for small $k_B\Delta$.

The asymptotic slopes for large $k_B\Delta$ and for small $k_B\Delta$ are +40 dB/decade and -40 dB/decade. For large $k_B\Delta$ the slope can be explained from equations (4.16). The value of $\min\left(\left|\omega^2\mathbf{M}_{ii}\right|/\left|\mathbf{K}_{ii}\right|\right)$ from equations (4.11) explains the asymptotic slope for small $k_B\Delta$ such that $\min\left(\left|\omega^2\mathbf{M}_{ii}\right|/\left|\mathbf{K}_{ii}\right|\right) = 1/420(k_B\Delta)^4$, which is related to $1/\omega^2$.

In this case, the transfer matrix results show marginally better accuracy. This is because the fact that the conditioned eigenvalue problem gives the repeated eigenvalues such that the method is more sensitive to perturbation [24]. For this example, the condition number of the matrices to be inverted in the transfer matrix approach and that in the conditioned eigenvalue problem is about same, as shown in Figure 4.5 (the peaks in the figure correspond to singularities in the matrix to be inverted). In addition, the matrix size is small $(n=4)$ such that the ill-conditioning of the eigenvalue problem is not so significant. Because of these reasons, the transfer matrix approach show better results.

Basically the same discussion holds for the relative errors in the eigenvectors. Figure 4.6 shows the relative errors in the rotational displacement of the eigenvector per unit displacement, which is analytically given by $|\theta/w|=k$ (e.g. [20,36]). The same trend as the relative error in the wavenumber can be seen.

The eigenvectors using the conditioned eigenvalue problem contain only displacement components such that force components are calculated using either equation (3.13) or (3.18). The shear force per unit displacement, which are analytically given by $|f/w|=EIk^3$ (e.g. [20,36]), are investigated. The relative errors in the shear force per unit displacement are plotted in Figure 4.7. The relative error associated with the transfer matrix approach shows the minimum especially at low frequencies because of the reason as stated previously. For the conditioned eigenvalue problem, the round-off error occurs through calculating either the original equation (3.13) or the SVD approach (3.18). It can be seen that the proposed SVD approach marginally reduces the relative errors especially at low frequencies where the round-off errors increase. Although the details are omitted, the same discussion holds for the moment component.

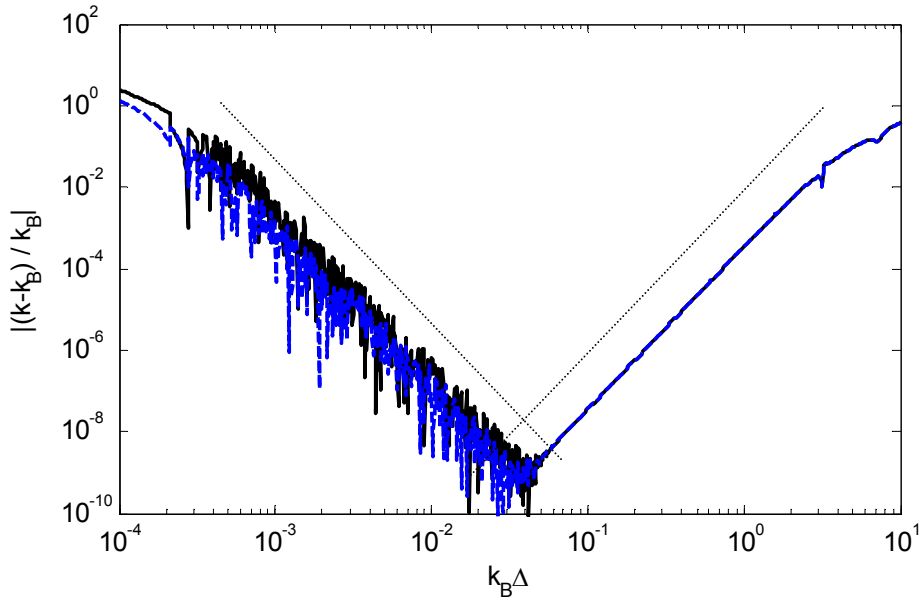

Figure 4.4: Relative errors in the propagation wavenumber for — the conditioned eigenvalue problem (3.9)*, – – the transfer matrix approach (2.15), ····· asymptote* $\pm 40 dB/decade$.

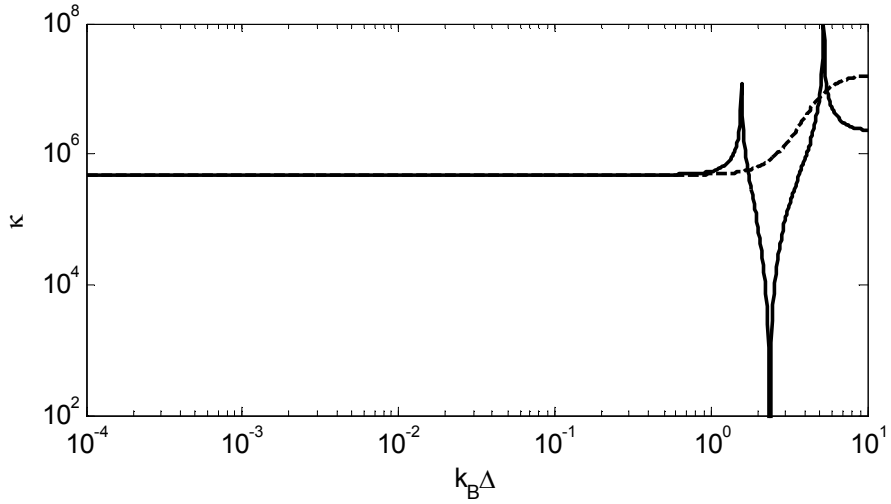

Figure 4.5: The condition numbers of (a) the matrix to be inverted: — the conditioned eigenvalue problem (3.9), – – the transfer matrix (2.15).

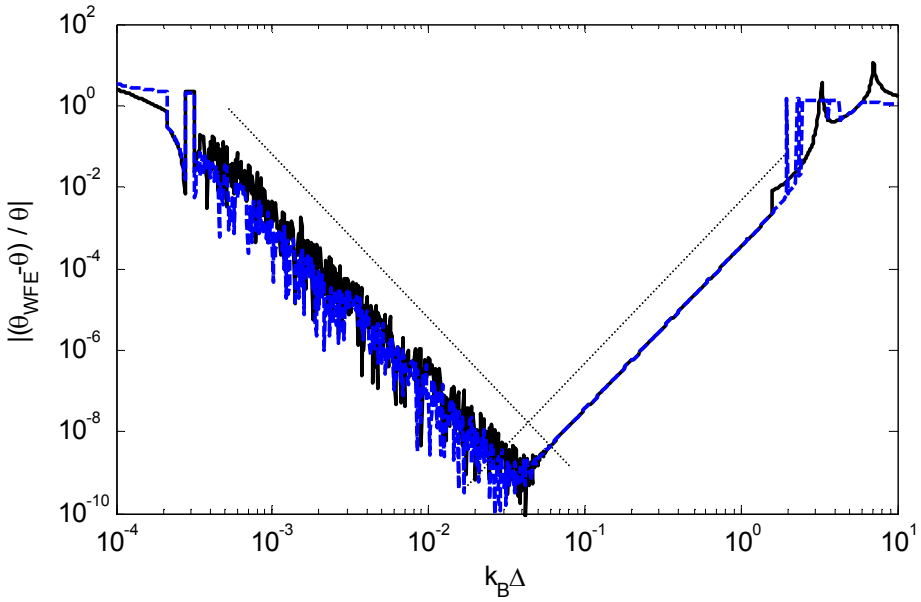

Figure 4.6: Relative errors in the rotational displacement per unit displacement: — the conditioned eigenvalue problem (3.9)*, – – the transfer matrix approach (2.15), ····· asymptote* $\pm 40 dB/decade$.

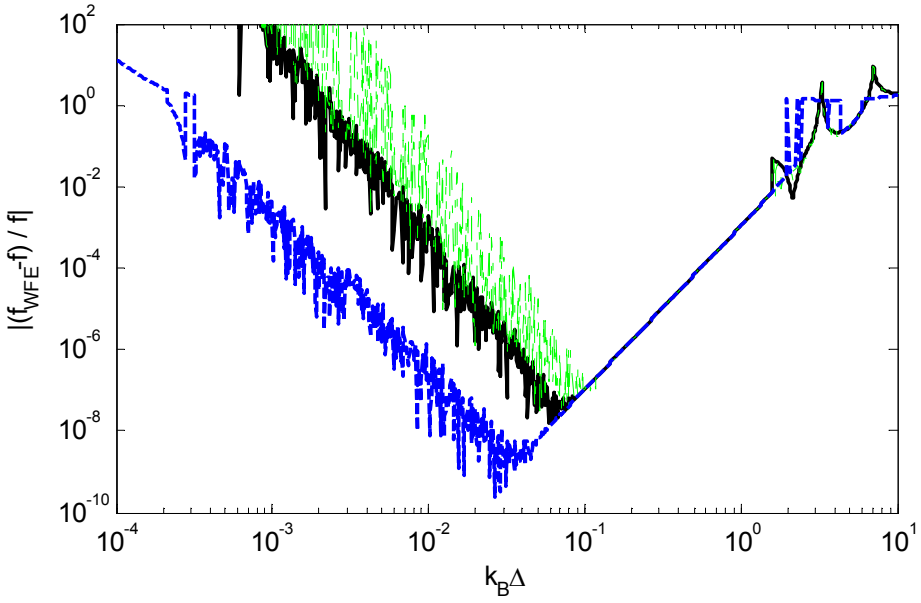

Figure 4.7: Relative errors in the shear force per unit displacement. Notation is same as Figure 4.7.

4.3.3 Relative Errors in the Group Velocity

The group velocity is numerically calculated using the methods outlined in Section 2.4. Figure 4.8 shows the relative error in the various estimates of the group velocity. The

analytical solution is given by $c_g = 2\omega/k_B$ (e.g. [21]). 1000 discretised frequencies are linearly taken in the log space of frequency.

The power and energy relationship and the differentiation of the eigenproblem show accurate results. The differentiation of the eigenproblem is likely to suffer from numerical errors because the method needs $\mathbf{D}_{LR}^{-1}$ to be evaluated and a large number of matrix operations such that numerical errors may accumulate. Smaller frequency step improves the accuracy of the result using the finite difference method for $k_B\Delta > 0.04$ and the error curve follows other two lines, which is the error bound given from the accuracy of the wavenumber.

Regardless of the methods, the numerical results show small errors for the range of, say, $0.01 \le k_B\Delta \le 1$ where both the eigenvalues and eigenvectors are accurately calculated. For the rod case, the range was about $10^{-6} \le k_L\Delta \le 1$. The difference of the lower bound results from the round-off errors due to the inertia term.

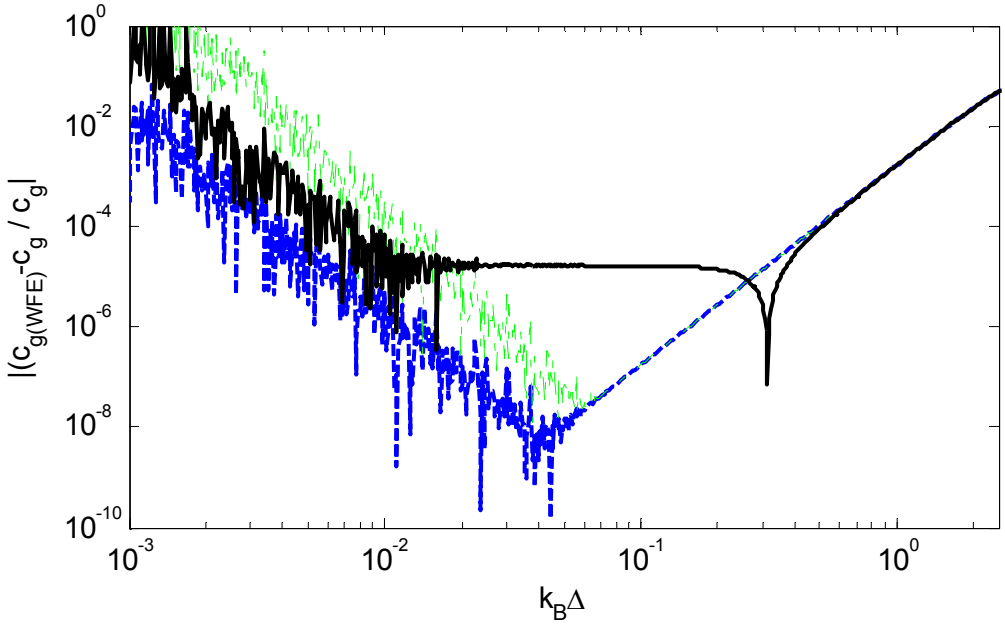

Figure 4.8: Relative errors in the group velocity: — finite difference, – – power and energy relationship, –·– differentiation of the eigenproblem.

5. NUMERICAL EXAMPLE OF A PLATE STRIP

5.1 Introduction

For two-dimensional structures, the conditioned eigenvalue problem should be applied to improve ill-conditioning occurring in the transfer matrix approach. Numerical examples are shown for flexural waves in a thin isotropic plate strip. No damping is assumed.

5.2 Analytical Expression for Flexural Waves in a Plate

A plate strip of width L_y, shown in Figure 5.1, is considered. The plate is thin and isotropic with simply supported boundary conditions along the *y*-wise plate edges. For such plate, the analytical wavenumber is given by [36]

$$k^2 = k_x^2 + k_y^2 = \pm\sqrt{\frac{\rho h}{D}}\omega \tag{5.1}$$

where $D = Eh^3 \big/ 12\left(1-\nu^2\right)$ is the bending rigidity, h is the thickness of the plate strip and ν is the Poisson's ratio. For the simply supported boundary condition along the plate edges $y = 0, L_y$, the wave modes have displacements proportional to $\sin\left(n\pi y / L_y\right)$ where n is an integer. The wavenumber along the *x*-direction is then given by

$$k_{xn}^2 = \pm\sqrt{\frac{\rho h}{D}}\omega - \left(\frac{n\pi}{L_y}\right)^2 \quad \left(n = 1, 2, \cdots\right). \tag{5.2}$$

Substituting $k_{xn} = 0$ into equation (5.2) gives the cut-off frequency for the nth wave as

$$\omega_n = \sqrt{\frac{D}{\rho h}}\left(\frac{n\pi}{L_y}\right)^2 \quad \left(n = 1, 2, \cdots\right). \tag{5.3}$$

The group velocity is given from equation (5.2) as

$$c_{gn} = \frac{\partial\omega}{\partial k_{xn}} = 2\sqrt{\frac{D}{\rho h}}k_{xn}. \tag{5.4}$$

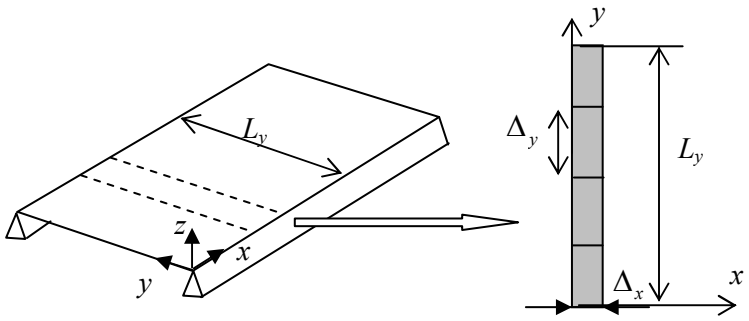

Figure 5.1: Simply supported plate strip.

5.3 Flexural Waves in a Plate Strip Using the WFE Method

The flexural waves in the plate strip are solved using the WFE method and results evaluated. In particular, reducing numerical errors is suggested using a FE model with internal nodes.

5.3.1 The WFE Formulation

The plate is assumed to be a steel plate with $L_y = 0.18$, $E = 2.0 \cdot 10^{11}$, $\rho = 7800$, $\nu = 0.30$ and $h = 1.8 \cdot 10^{-3}$, all in SI units. The mass and stiffness matrices are formed using ANSYS 7.1. A four node plane strain shell element (SHELL63), which uses cubic polynomial shape functions for both the *x*- and *y*-directions, was chosen. The aspect ratio of FE $\gamma = \Delta_x / \Delta_y \approx 1$ is preferable since $k_x \Delta_x \leq 1$ and $k_y \Delta_y \leq 1$ should be satisfied.

5.3.2 Results Using the Transfer Matrix

The ill-conditioning of the transfer matrix approach is illustrated in this section. Consider a plate strip model comprising 4 elements as shown in Figure 5.2. After removing the in-plane DOFs and DOFs associated with the boundary conditions, there are 22 resulting DOFs for the model. Since the *y*-wise wavenumber is $k_y = n\pi / L_y$ for the *n*th wave mode, only the *n*=1 wave mode could be expected to be accurate since $k_y \Delta_y = \pi / 4 \left(< 1 \right)$.

The dispersion relationships are shown in Figures 5.3. The abscissa represents the non-dimensional frequency $\Omega = L_y^2 / \pi^2 \sqrt{\rho h / D}\, \omega$ and the cut-off frequencies occur at $\Omega = n^2$ (*n*=1,2,3…). The ordinate shows the non-dimensional wavenumber, $k_x L_y / \pi$, which becomes

-jn for the *n*th mode at $\Omega = 0$. When $k_x \Delta_x = 1$ then $k_x L_y / \pi = 3.18$, so that the FE discretisation error should be small if $\left| k_x L_y / \pi \right| < 3.18$.

The wavenumber calculated from the transfer matrix (2.15) and that from the conditioned eigenvalue problem (3.9) are shown in Figure 5.3 (a) and (b), respectively. There are two waves associated with the *n*=1 mode. One is a propagating wave which cuts-on at $\Omega = 1$ and another is a nearfield wave. In Figure 5.3 (a), it can be seen that the wave near the cut-off frequency $(\Omega = 1)$ is inaccurate. This is because the two roots associated with the positive and negative going wave are such that $e^{\pm jkx} \to 1$ around the cut-off frequency and such roots are likely to be estimated inaccurately because of the ill-conditioning. In turn, relatively accurate results are obtained for the conditioned eigenvalue problem in Figure 5.3 (b) because of the conditioning described in Section 3.

The condition numbers of the matrices to be inverted ($\mathbf{D}_{LR}$ in equation (2.14) and $\mathbf{Z}_2$ in equation (3.9)) and those of the eigenvalue problems ($\mathbf{T}$ in equation (2.15) and $\mathbf{Z}_2^{-1}\mathbf{Z}_1$ in equation (3.9)) are plotted in Figures 5.4. Both the condition number for the matrix to be inverted in Figure 5.4 (a) and that for the eigenvalue problem in Figure 5.4 (b) are worse-conditioned when the transfer matrix approach is used. The condition numbers are almost constant in this frequency range of interest. For plate strip models with more elements, the numerical artefact around the cut-off frequency becomes more prominent because of the worse conditioning and the results using the transfer matrix approach will completely break down.

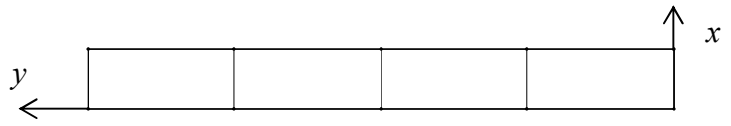

Figure 5.2: The plate strip FE model, $\Delta_x = 18mm, \Delta_y = 45mm\left(L_y/4\right)$.

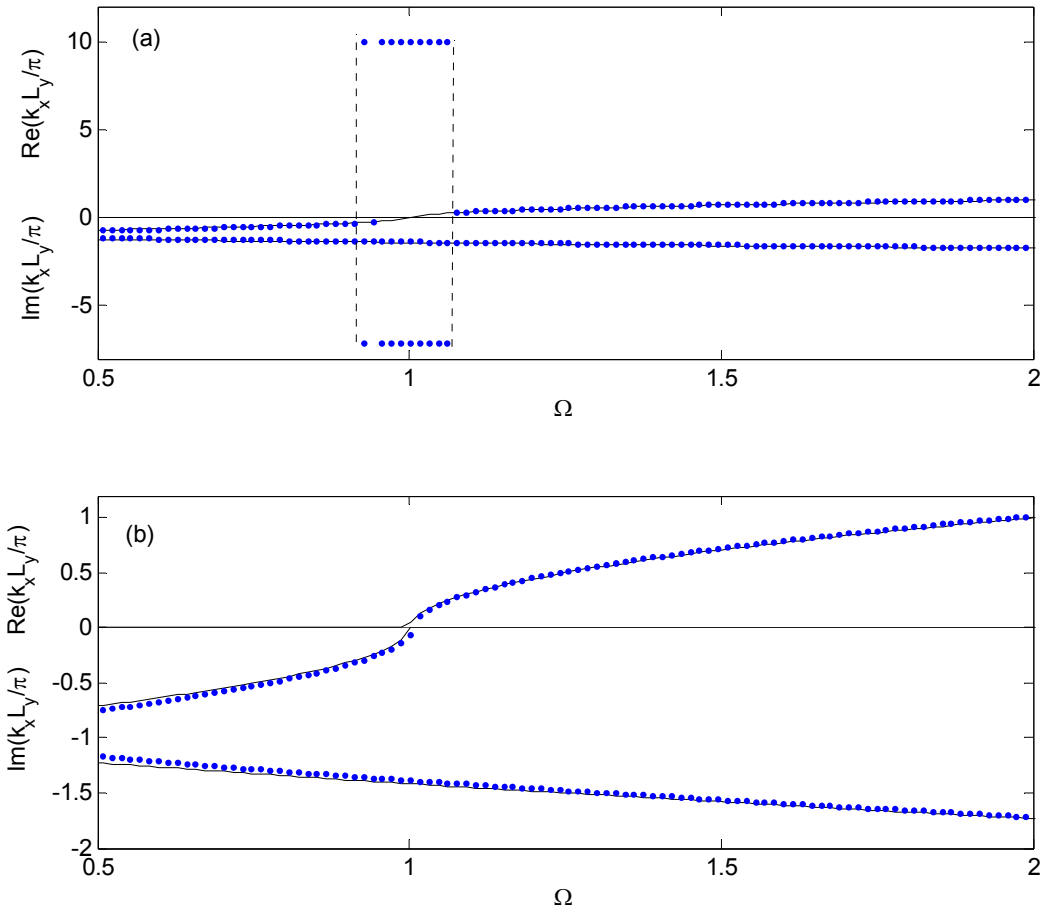

Figures 5.3: Dispersion relationships: — analytical solution, ···· the WFE result using (a) the transfer matrix approach, (b) the conditioned eigenvalue problem.

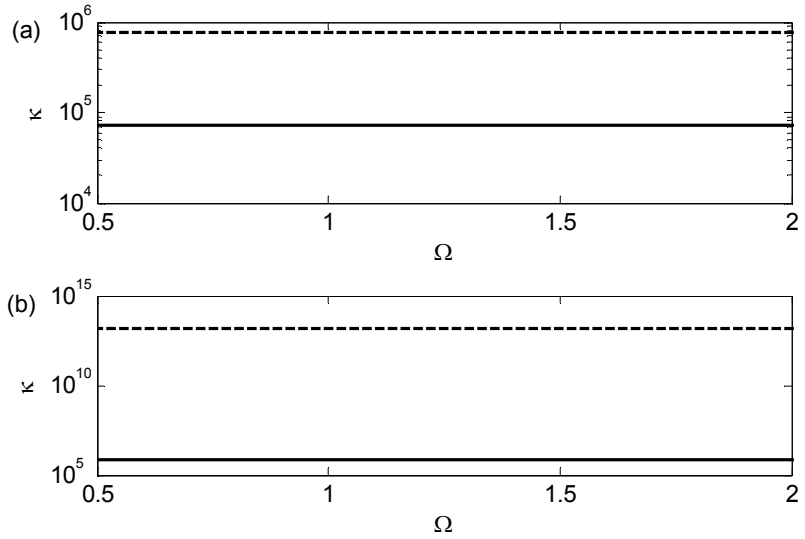

Figures 5.4: The condition numbers of (a) the matrices to be inverted, (b) the eigenvalue problems: – – the transfer matrix approach, — the conditioned eigenvalue problem.

5.3.3 Relationship between the Condition Number and Matrix Size

Even for the conditioned eigenvalue problem, the conditioning is still of concern. The condition number κ of the matrix to be inverted is discussed in this section. For flexural waves in a plate strip, the condition number of $\mathbf{Z}_2$ in equation (3.9) is examined. If κ is large, numerical errors occur when the matrix is inverted and the resulting eigenvalue problem is likely to be numerically contaminated.

The condition number depends on the modelling of the plate strip model. Here κ are determined for several plate strip models and the results are shown in Figure 5.5. It can be seen that as (1) Δ_x becomes smaller and (2) the matrix size increases and (3) the aspect ratio γ of the element becomes large, κ increases. From the figure, the relationships between κ, Δ and the number of elements, *N*, are approximately expressed as

$$\kappa \propto \Delta_x^{-2} \quad \text{or} \quad \kappa \propto N^2 \tag{5.5}$$

for the same element aspect ratio. As the number of elements increases, the condition number gets larger because the number of the singular values of the matrix increases which usually results in there being a wider range of the relative magnitudes of the singular values.

Next the effect of the aspect ratio, γ, is determined for the same element area as Figure 5.6. The case of $\gamma = 0.2$ is also included. For elements of the same area, the dependence in γ is shown in Figure 5.7. The ordinate shows the ratio of κ to that for $\gamma = 1$. From the figure, the relationships between γ and κ are roughly estimated as

$$\kappa / \kappa_{\gamma=1} \propto \gamma^{2.1} \left(\gamma > 1\right), \quad \kappa / \kappa_{\gamma=1} \propto \gamma^{-0.4} \left(\gamma < 1\right) \tag{5.6}$$

such that rectangular elements $\left(\gamma \neq 1\right)$ cause κ to be larger. The condition number of the matrix to be inverted is usually related to $\kappa\left(\mathbf{D}_{LR}\right)$. The matrix $\mathbf{D}_{LR}$ represents the relationship between forces and displacements across an element, i.e. $\mathbf{f}_L = \mathbf{D}_{LR}\mathbf{x}_R$. When the range of the magnitude of elements in $\mathbf{D}_{LR}$ increases, the condition number often deteriorates. For elements with $\gamma \neq 1$, only some elements become large compared to others. More detail expression of the effect of γ in $\mathbf{D}_{LR}$ can be seen in [35]. Some elements approach infinity with different coefficients for the limiting case of $\gamma \to \infty$ or $\gamma \to 0$ such that $\kappa\left(\mathbf{D}_{LR}\right)$ deteriorates.

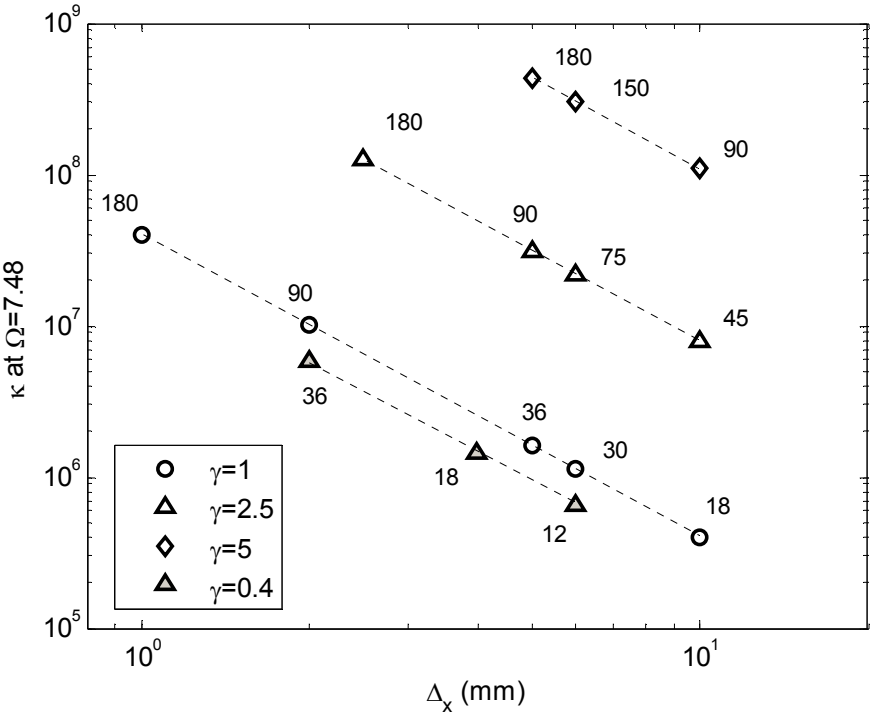

Figure 5.5: Condition numbers of the matrix to be inverted at $\Omega = 7.48$. Each number in the figure denotes the numbers of elements.

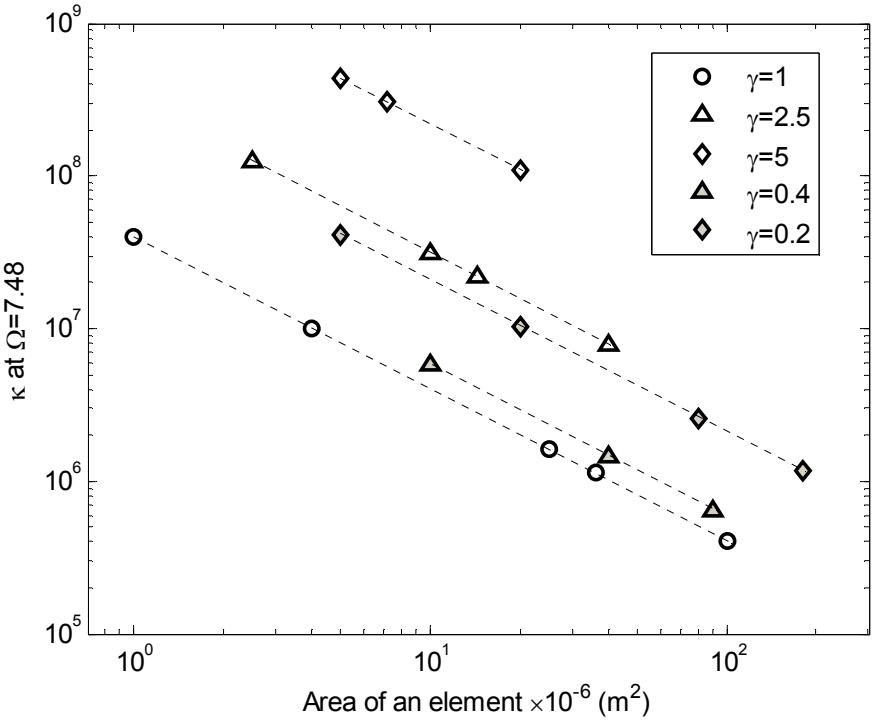

Figure 5.6: Condition numbers as a function of the area of an element.

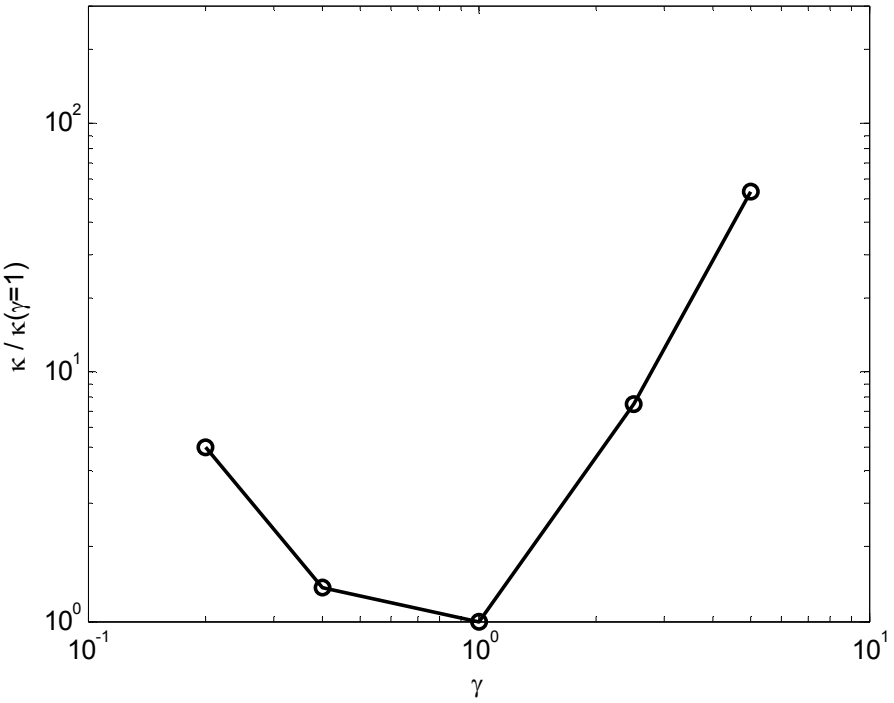

Figure 5.7: Condition number as a function of the aspect ratio.

5.3.4 Relative Error in the Eigenvalues and Eigenvectors

Based on the previous discussions, the relative error in the eigenvalues is investigated using the conditioned eigenvalue problem. An 18 elements $\left(\Delta_x = \Delta_y = 10mm\right)$ plate strip model is first evaluated. The dispersion relationship is shown in Figure 5.8. For the model, $k_x\Delta_x = 1$ is associated with $k_xL_y/\pi = 5.73$ and $k_y\Delta_y = 1.05$ for the *n*=6 wave mode.

Six wave modes cut on in the frequencies analysed. The dispersion relationship shows that the WFE results generally agree well with the analytical solution. Some discrepancies can be seen for higher wave modes and for large $\left|k_xL_y/\pi\right|$ as the FE discretisation errors (and the round-off error due to the inertia term at low frequencies) increase. At low frequencies, two nearfield waves calculated in the WFE method become complex conjugate pairs as a numerical artefact. The real part is small compared to the imaginary part by a factor of about 10. In the figure, only the imaginary part is plotted for clarity.

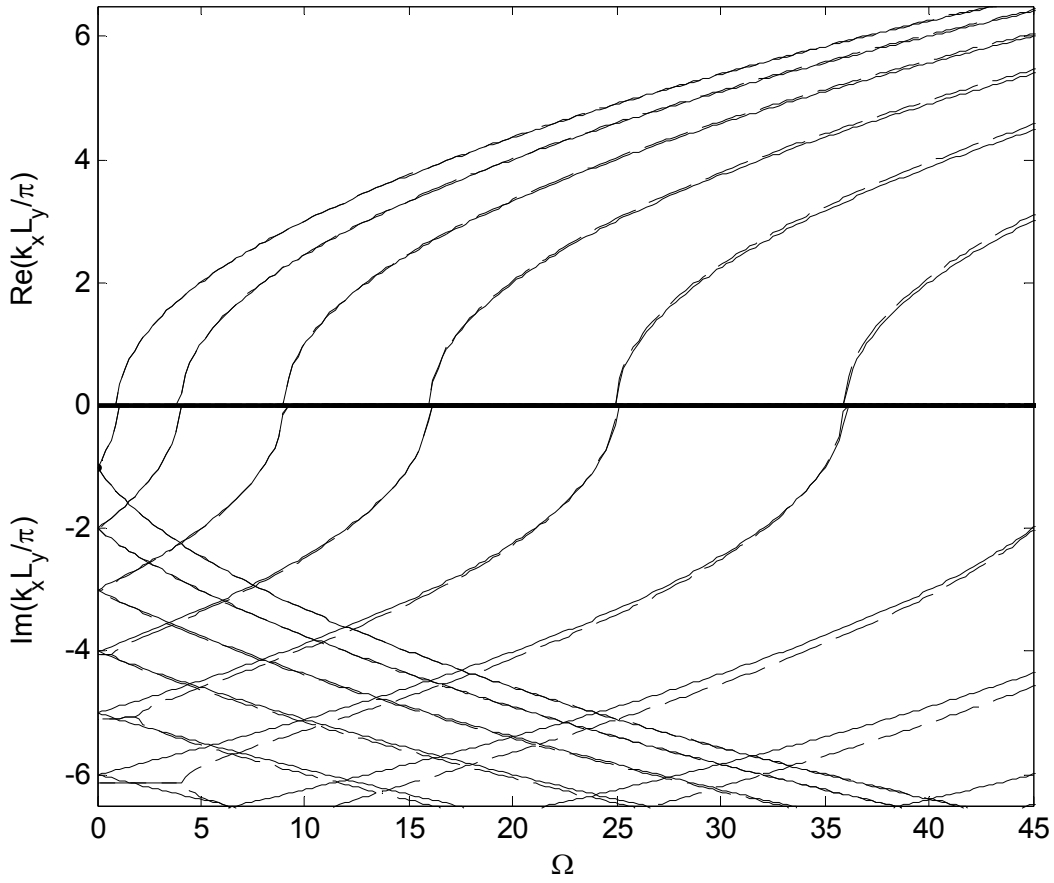

Figure 5.8: Dispersion relationship for the 18 element plate strip $\left(\Delta_x = \Delta_y = 10mm\right)$*: — analytical solution, – – WFE result.* $\left(k_x\Delta_x\big|_{\max} \approx 1.16\right)$.

The relative error in the wavenumber associated with the *n*=1 mode is shown in Figure 5.9. The results are shown for three FE models, which are the 18 elements $\left(\Delta_x = \Delta_y = 10mm\right)$, 36 elements $\left(\Delta_x = \Delta_y = 5mm\right)$ and 90 elements $\left(\Delta_x = \Delta_y = 2mm\right)$ plate strip models. The peaks at the cut-off frequency $\left(\Omega = 1\right)$ occur because the denominator approaches 0 $\left(k \to 0\right)$. The FE discretisation errors become smaller for the smaller Δ_x FE models. However, the round-off errors due to the inertia term increase at low frequencies for small Δ (the 90 elements model). For the 90 elements model, $k_x\Delta_x$ becomes 1 around $\Omega = 900$.

Similarly, the relative errors in the eigenvector (the rotational displacement per unit displacement $\left(\theta/w\right)$) associated with the *n*=1 wave are shown in Figure 5.10. A similar trend

to the eigenvalue can be seen. The relative error in the eigenvector is generally larger than that in the eigenvalues for large matrix size as can be seen also in this case.

The shear force is next evaluated using the SVD approach (3.18). The analytical expression for the shear force is [36]

$$\tau/w = jDk_x\left(k_x^2 + (2-\nu)k_y^2\right). \tag{5.7}$$

The relative error in the calculated shear force per unit translational displacement (τ/w) is shown in Figure 5.11. It can be seen that the errors associated with the 18 and 36 elements model are similar to that in the wavenumbers and eigenvectors. However, the error associated with the 90 elements model is large because (1) $k_x\Delta_x$ is small such that $\lambda \approx 1$ in equation (3.19) causes the round-off errors in arithmetic calculation and (2) the matrix size is large such that round-off errors may accumulate.

The SVD approach for numerically determining the eigenvector reduces the numerical error. Although the error in each eigenvalue component (w,θ) is small, the error in τ can be substantial. Figure 5.12 shows the relative error in τ/w using the original approach (3.13) and the SVD approach (3.18). It can be seen that the relative error associated with the SVD approach is generally smaller especially at low frequencies and around the cut-off frequency where the round-off error through the matrix operations in the original approach (3.13) is likely to occur.

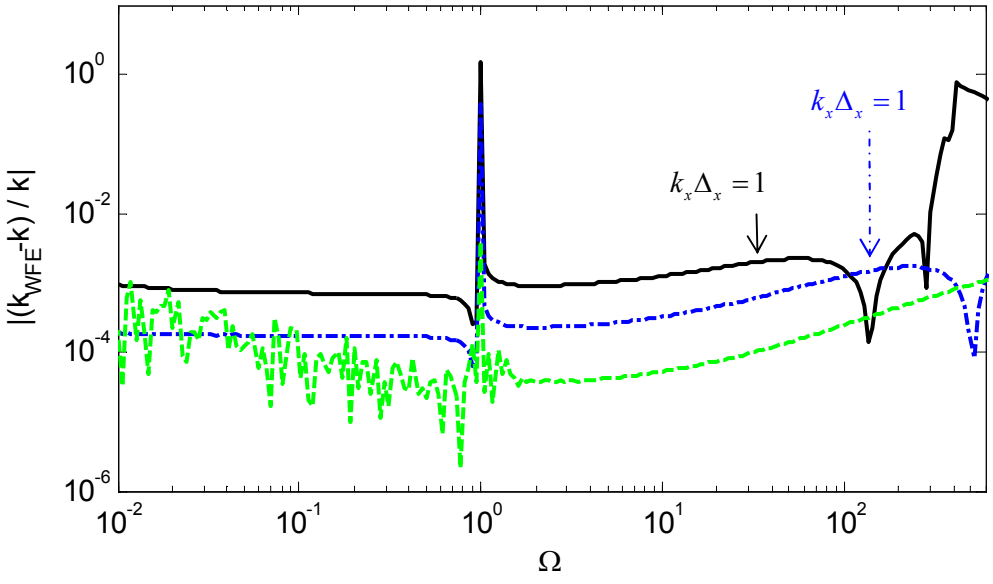

Figure 5.9: Relative errors in the wavenumber for the n=1 mode: — the 18 elements, –·– 36 elements, – – 90 elements plate strip model.

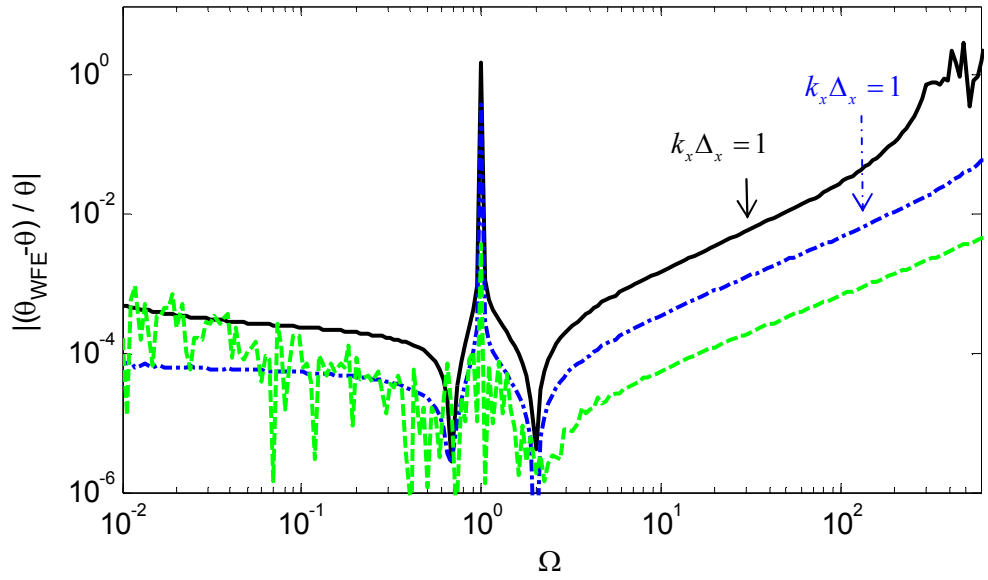

Figure 5.10: Relative errors in θ/w in the eigenvector. Notation is same as Figure 5.9.

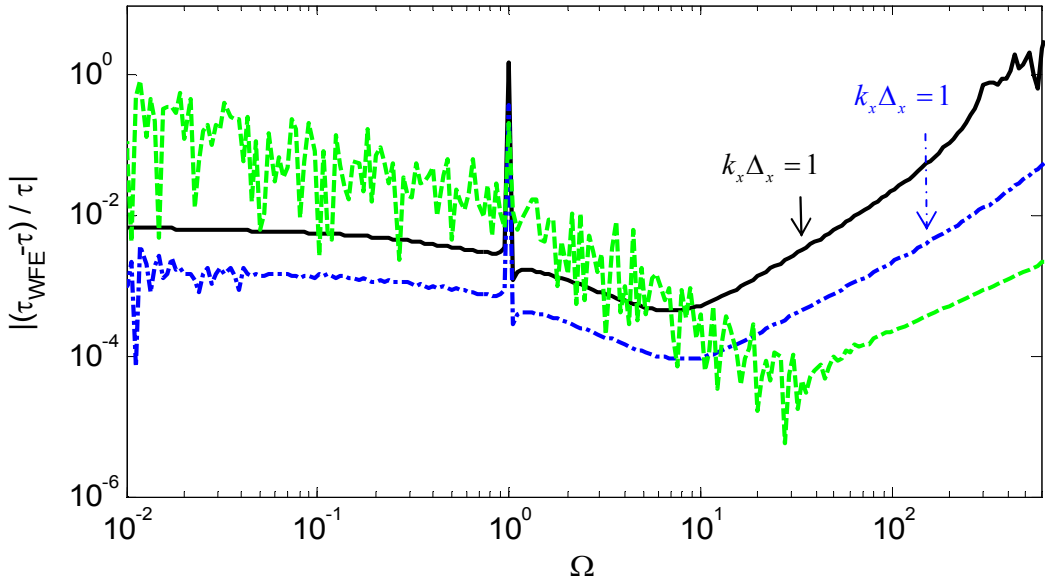

Figure 5.11: Relative errors in τ/w in the eigenvector. Notation is same as Figure 5.9.

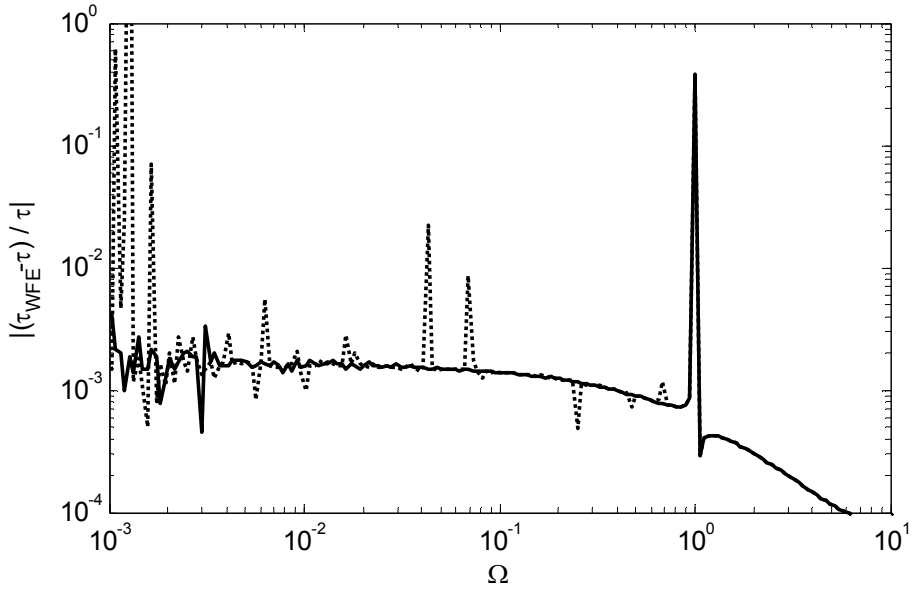

Figure 5.12: Relative errors in τ/w in the eigenvector: — the SVD approach, ····· the original approach.

5.3.5 Reducing Numerical Errors Using a FE Model with Internal Nodes

There is a clear trade-off among the round-off errors due to the inertia term, the FE discretisation error and the conditioning especially at low frequencies. To calculate accurate results at low frequencies, using internal nodes for the FE model (two or more series of elements jointed together) as shown in Figure 5.13 can be used. After the DOFs associated with internal nodes are condensed using equation (2.7), the resulting FE model can reduce both the round-off error due to the inertia term and the FE discretisation error because the length Δ is increased and more accurate shape function is equivalently applied in the direction of wave propagation after removing the DOFs associated with internal nodes. By using this approach, the trade-off can be alleviated. The number of rows for internal nodes can be more than 1 but care should be taken because the large condition number of $\mathbf{D}_{II}$ in equation (2.8) may cause another numerical error.

The relative error in the wavenumber for the n=1 mode is shown in Figure 5.14. The results using a FE model with one row of internal nodes $\left(\Delta_x = 4mm, \Delta_y = 2mm\right)$ are compared with the original FE model $\left(\Delta_x = \Delta_y = 2mm\right)$. In addition, results using a model of 90 rectangular

elements $\left(\Delta_x = 4mm, \Delta_y = 2mm\right)$ without internal nodes are also shown. It can be seen that the relative error for the model with internal nodes is reduced especially at low frequencies.

Table 5.1 shows the value of $\left|\mathbf{M}_{ii}\right| / \left|\mathbf{K}_{ii}\right|$ associated with τ, m_x, m_y (the DOFs associated with flexural motion) for small Ω. Especially for DOFs associated with the moment m_y, the value is increased because of the increase in Δ_x so that the round-off error due to the inertia is reduced for the model with internal nodes and the model with rectangular elements. Since Δ_y is same for all FE models, $\min\left(\left|\omega^2\mathbf{M}_{ii}\right| / \left|\mathbf{K}_{ii}\right|\right)$ is about same for the models as can be seen from Table 5.1 (elements associated with m_x). Figure 5.15 shows $\min\left(\left|\omega^2\mathbf{M}_{ii}\right| / \left|\mathbf{K}_{ii}\right|\right)$ for the model with internal nodes as a function of Ω as a rough estimate of the round-off errors. All the models typically show similar results to Figure 5.15.

Similarly, the relative error in τ / w is considered. The results using the 90 element model $\left(\Delta_x = \Delta_y = 2mm\right)$ is poor (Figure 5.11) because of the round-off error due to the inertia term and the small value of $k_x\Delta_x$ $\left(\lambda \approx 1\right)$. These errors can be improved using the model with internal nodes. Results using the model with internal nodes are shown in Figure 5.16. It can be seen that the FE model using internal nodes can greatly improve accuracy of the result.

The condition number $\kappa\left(\mathbf{D}_{II}\right)$ for the FE model using internal nodes is about 10^{13} in the frequency range of interest and the pseudo-matrix inverse is applied. Even for such a large condition number, it is seen that a FE model with internal nodes reduces numerical errors.

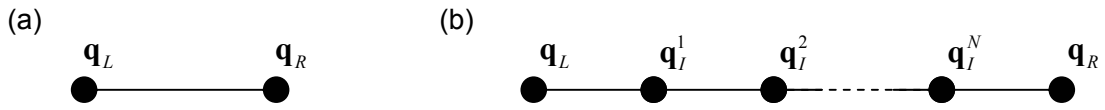

Figures 5.13: (a) Single element, (b) multiple elements with N series of internal nodes to be concentrated.

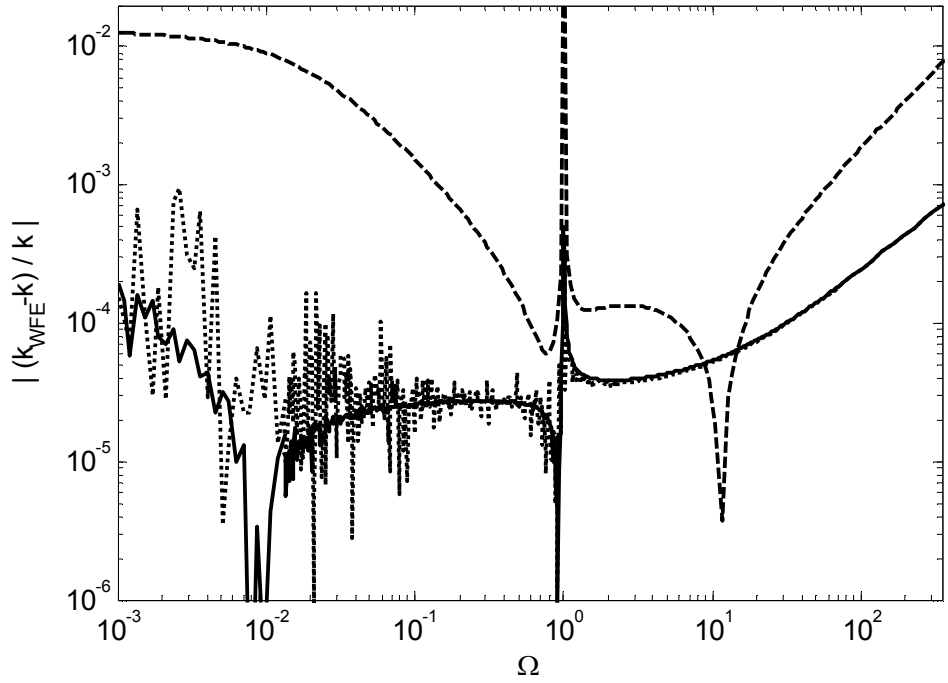

Figure 5.14: Relative errors in the wavenumber for the n=1 mode: ····· original FE model, — FE model with internal nodes, – – rectangular FE model.

	Single element set $\left(\Delta_x = \Delta_y = 2mm\right)$	Two series of elements (with internal nodes) $\left(\Delta_x = 4mm, \Delta_y = 2mm\right)$	Single element set $\left(\Delta_x = 4mm, \Delta_y = 2mm\right)$
m_x, θ_x	4.82×10^{-15}	5.24×10^{-15}	5.92×10^{-15}
m_y, θ_y	4.82×10^{-15}	3.42×10^{-14}	5.70×10^{-14}
τ, w	3.14×10^{-14}	7.64×10^{-14}	7.74×10^{-14}

Table 5.1: $\left|\mathbf{M}_{ii}\right| / \left|\mathbf{K}_{ii}\right|$ *associated with each DOF.*

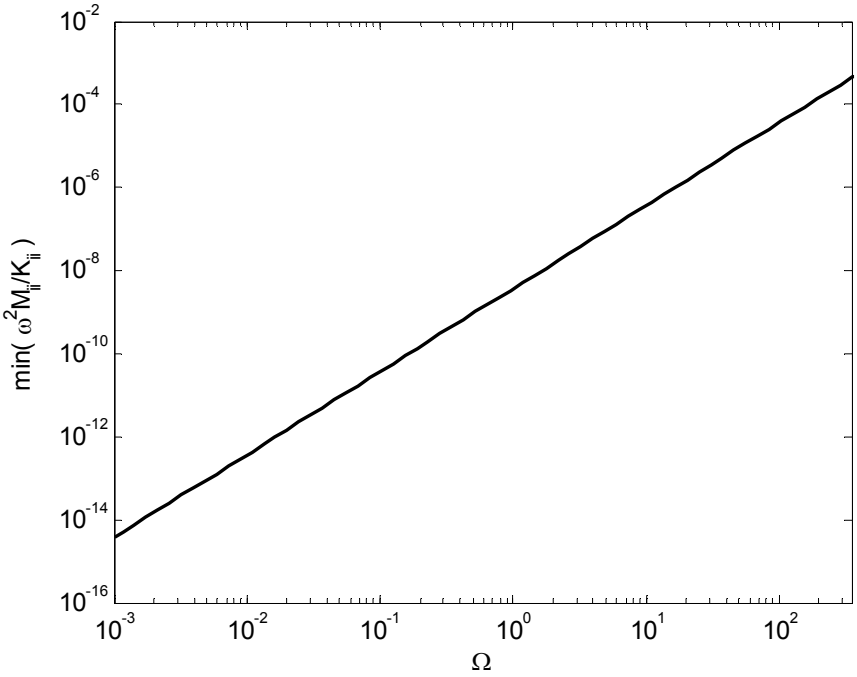

Figure 5.15: $\min\left(\left|\omega^2\mathbf{M}_{ii}\right|/\left|\mathbf{K}_{ii}\right|\right)$ *as a function of* Ω.

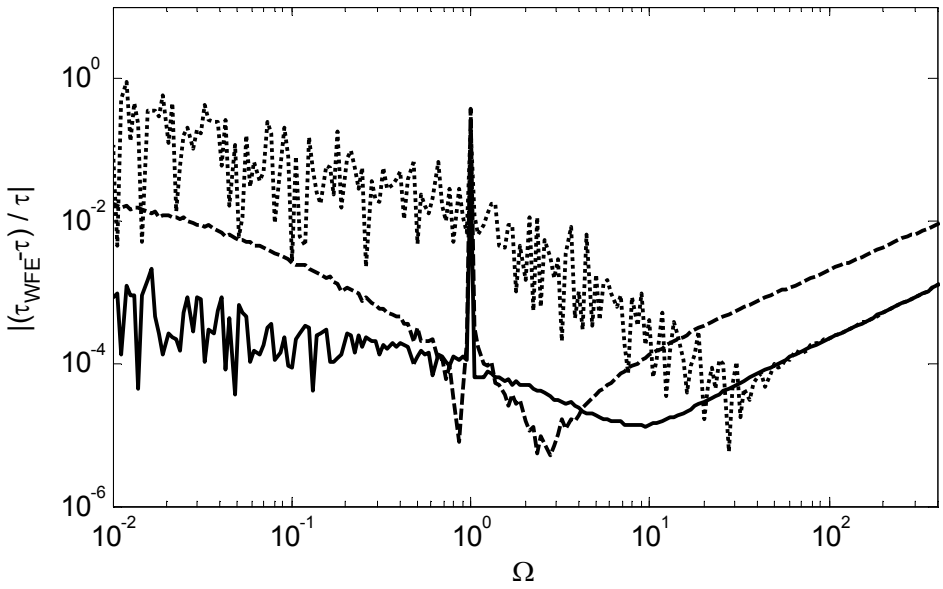

Figure 5.16: Relative errors in τ/w *in the eigenvector: ····· original FE model, — FE model with internal nodes, – – rectangular FE model.*

5.3.6 Condensation Using Approximate Expressions

In Section 5.3.5, the FE model using internal nodes has been validated and good improvement in numerical errors has been shown. However, the method needs the matrix inverse $\mathbf{D}_{II}^{-1}$ in equation (2.8) to be evaluated at each frequency and hence the calculation cost is high. In addition, round-off errors may be large in the calculation of the elements of the dynamic stiffness matrix. It should be noted that this section focuses on reducing round-off errors in numerical calculations for elements of the dynamic stiffness matrix, not for the inertia term. $\mathbf{D}_{II}^{-1}$ can be expressed as

$$\mathbf{D}_{II}^{-1} = \left(\mathbf{K}_{II} - \omega^2 \mathbf{M}_{II}\right)^{-1} = \left(\mathbf{I} - \omega^2 \mathbf{K}_{II}^{-1}\mathbf{M}_{II}\right)^{-1} \mathbf{K}_{II}^{-1} \tag{5.8}$$

where $\mathbf{M}_{II}, \mathbf{K}_{II}$ are the elements of the mass and stiffness matrices associated with internal DOFs. For small $\mathbf{K}_{II}^{-1}\mathbf{M}_{II}$ a series expansion can be applied, i.e. to the first order

$$\mathbf{D}_{II}^{-1} = \mathbf{K}_{II}^{-1} + O\left(\mathbf{K}_{II}^{-1}\mathbf{M}_{II}\right) \tag{5.9}$$

or, to the second order,

$$\mathbf{D}_{II}^{-1} = \left(\mathbf{I} + \omega^2 \mathbf{K}_{II}^{-1}\mathbf{M}_{II}\right)\mathbf{K}_{II}^{-1} + O\left(\mathbf{K}_{II}^{-1}\mathbf{M}_{II}\right)^2. \tag{5.10}$$

Equations (5.9) and (5.10) need only $\mathbf{K}_{II}^{-1}$ to be evaluated such that the calculation cost is low.

For clarity, equation (5.9) is referred to the 1st order approximation and equation (5.10) is referred to the 2nd order approximation while the original approach is referred as dynamic condensation. Using equations (5.9) and (5.10), the original equation (2.8) and the associated mass and stiffness matrices (for the calculation of the group velocity) can be derived.

For the 1st order approximation (5.9), the condensation (2.8) becomes

$$\mathbf{D}_{MM} - \mathbf{D}_{MI}\mathbf{D}_{II}^{-1}\mathbf{D}_{IM} \approx \mathbf{K}_{MM} - \mathbf{K}_{MI}\mathbf{K}_{II}^{-1}\mathbf{K}_{IM} - \omega^2\left(\mathbf{M}_{MM} - \mathbf{K}_{MI}\mathbf{K}_{II}^{-1}\mathbf{M}_{IM} - \mathbf{M}_{MI}\mathbf{K}_{II}^{-1}\mathbf{K}_{IM}\right). \tag{5.11}$$

The associated mass and stiffness matrices become

$$\begin{aligned} \mathbf{R}^{\mathrm{T}}\mathbf{K}\mathbf{R} &\approx \mathbf{K}_{MM} - \mathbf{K}_{MI}\mathbf{K}_{II}^{-1}\mathbf{K}_{IM}, \\ \mathbf{R}^{\mathrm{T}}\mathbf{M}\mathbf{R} &\approx \mathbf{M}_{MM} - \mathbf{K}_{MI}\mathbf{K}_{II}^{-1}\mathbf{M}_{IM} - \mathbf{M}_{MI}\mathbf{K}_{II}^{-1}\mathbf{K}_{IM}. \end{aligned} \tag{5.12}$$

It can be seen that the large terms associated with the stiffness and the small terms associated with the inertia are appropriately grouped such that the round-off errors in the arithmetic operation can be reduced.

Similarly, the 2nd order approximation (5.10) gives

$$\begin{aligned}\mathbf{D}_{MM}-\mathbf{D}_{MI}\mathbf{D}_{II}^{-1}\mathbf{D}_{IM} \approx{}& \mathbf{K}_{MM}-\mathbf{K}_{MI}\mathbf{K}_{II}^{-1}\mathbf{K}_{IM}\\ &-\omega^2\left(\mathbf{M}_{MM}-\mathbf{K}_{MI}\mathbf{K}_{II}^{-1}\mathbf{M}_{IM}-\mathbf{M}_{MI}\mathbf{K}_{II}^{-1}\mathbf{K}_{IM}+\mathbf{K}_{MI}\mathbf{K}_{II}^{-1}\mathbf{M}_{II}\mathbf{K}_{II}^{-1}\mathbf{K}_{IM}\right)\\ &-\omega^4\left(\mathbf{M}_{MI}\mathbf{K}_{II}^{-1}\mathbf{M}_{IM}-\mathbf{K}_{MI}\mathbf{K}_{II}^{-1}\mathbf{M}_{II}\mathbf{K}_{II}^{-1}\mathbf{M}_{IM}-\mathbf{M}_{MI}\mathbf{K}_{II}^{-1}\mathbf{M}_{II}\mathbf{K}_{II}^{-1}\mathbf{K}_{IM}\right)\end{aligned} \tag{5.13}$$

and

$$\begin{aligned}\mathbf{R}^{\mathrm{T}}\mathbf{K}\mathbf{R} \approx{}& \mathbf{K}_{MM}-\mathbf{K}_{MI}\mathbf{K}_{II}^{-1}\mathbf{K}_{IM}\\ &+\omega^4\left(\mathbf{M}_{MI}\mathbf{K}_{II}^{-1}\mathbf{M}_{IM}-\mathbf{K}_{MI}\mathbf{K}_{II}^{-1}\mathbf{M}_{II}\mathbf{K}_{II}^{-1}\mathbf{M}_{IM}-\mathbf{M}_{MI}\mathbf{K}_{II}^{-1}\mathbf{M}_{II}\mathbf{K}_{II}^{-1}\mathbf{K}_{IM}\right),\\ \mathbf{R}^{\mathrm{T}}\mathbf{M}\mathbf{R} \approx{}& \mathbf{M}_{MM}-\mathbf{K}_{MI}\mathbf{K}_{II}^{-1}\mathbf{M}_{IM}-\mathbf{M}_{MI}\mathbf{K}_{II}^{-1}\mathbf{K}_{IM}+\mathbf{K}_{MI}\mathbf{K}_{II}^{-1}\mathbf{M}_{II}\mathbf{K}_{II}^{-1}\mathbf{K}_{IM}\\ &+2\omega^2\left(\mathbf{M}_{MI}\mathbf{K}_{II}^{-1}\mathbf{M}_{IM}-\mathbf{K}_{MI}\mathbf{K}_{II}^{-1}\mathbf{M}_{II}\mathbf{K}_{II}^{-1}\mathbf{M}_{IM}-\mathbf{M}_{MI}\mathbf{K}_{II}^{-1}\mathbf{M}_{II}\mathbf{K}_{II}^{-1}\mathbf{K}_{IM}\right).\end{aligned} \tag{5.14}$$

Using these two approximations, the relative errors in the wavenumber are evaluated and compared with the result using dynamic condensation (as shown in Figure 5.14). The result is shown in Figure 5.17. The relative error for the 1st order approximation is poor at high frequencies and becomes about 1 % at $\Omega=10^{-1}$ where $\min\left(\left|\omega^2\mathbf{M}_{ii}\right|/\left|\mathbf{K}_{ii}\right|\right)$ is 10^{-10} as seen from Figure 5.15. In the frequency range analysed, the 2nd order approximation gives good results as shown in Figure 5.18, with accuracy comparable to that using the dynamic condensation.

For the frequencies where $\left|\omega^2\mathbf{M}_{ij}\right|/\left|\mathbf{K}_{ij}\right|$ is small enough, the 2nd order approximation, equations (5.13) and (5.14), is recommended to reduce round-off errors in arithmetic calculations and to reduce the calculation cost. Since $\left|\omega^2\mathbf{M}_{ij}\right|/\left|\mathbf{K}_{ij}\right|$ is small enough, $\kappa\left(\mathbf{K}_{II}\right)$ is about same as $\kappa\left(\mathbf{D}_{II}\right)$ as shown in Figure 5.19.

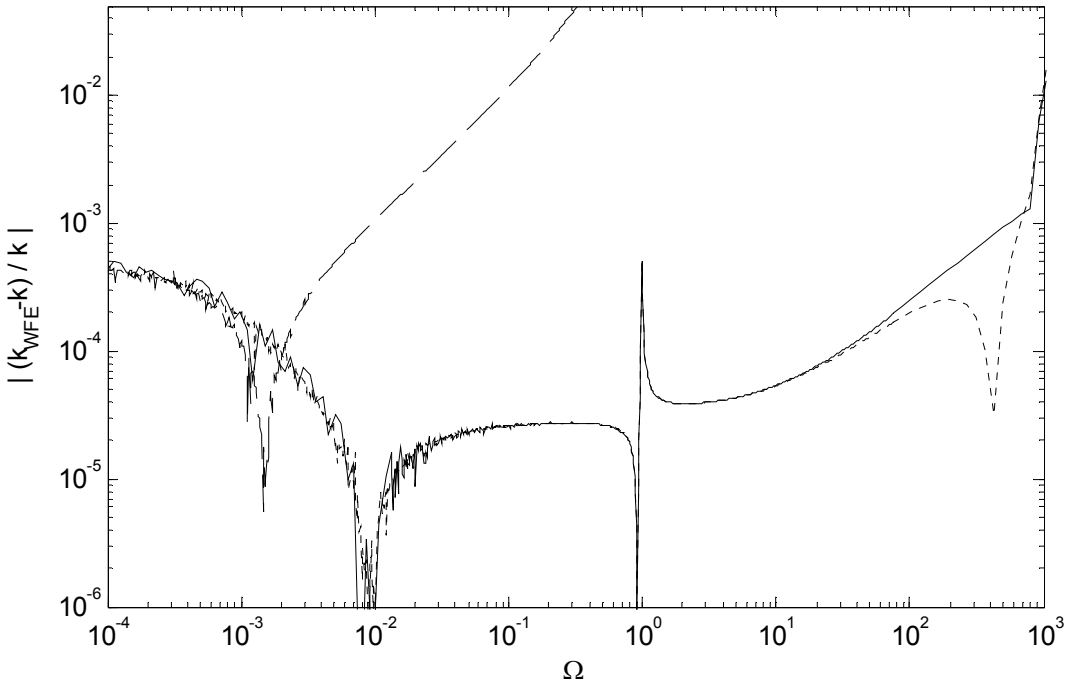

Figure 5.17: Relative errors in the wavenumber for the n=1 mode: — dynamic condensation, – – the 1st order approximation, ····· the 2nd order approximation.

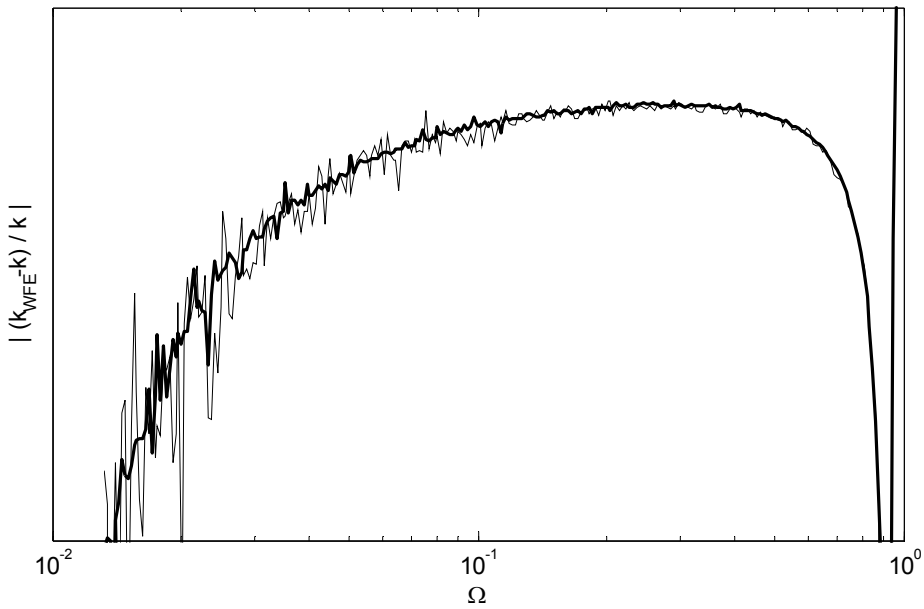

Figure 5.18: Relative errors in the wavenumber for the n=1 mode: — (thin) dynamic condensation, — (thick) the 2nd order approximation.

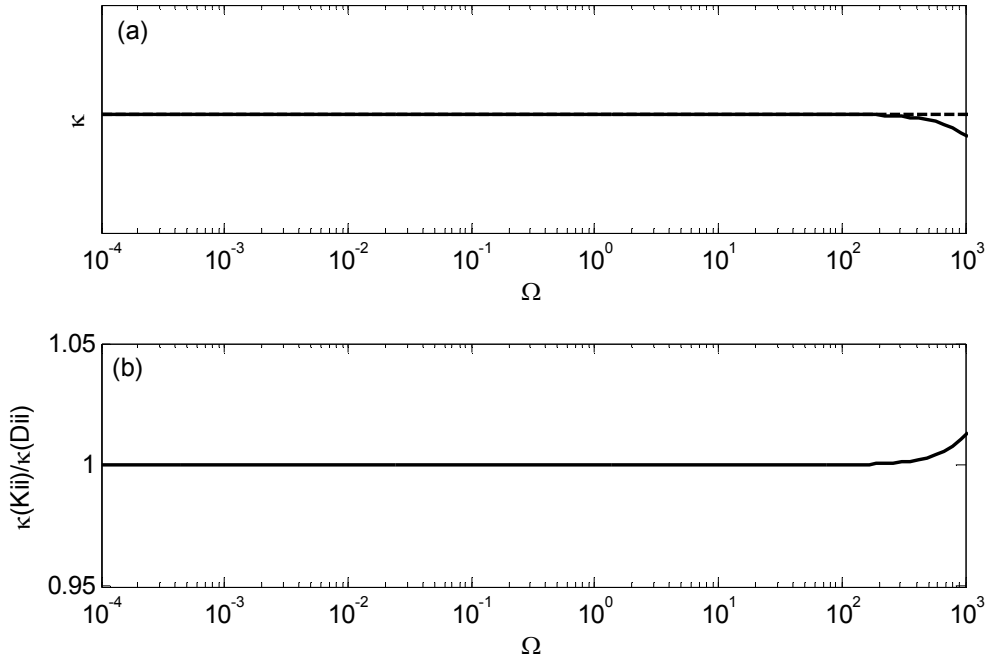

Figure 5.19: (a) Condition numbers: — $\kappa(\mathbf{D}_{II})$, -- $\kappa(\mathbf{K}_{II})$. *(b)* $\kappa(\mathbf{K}_{II})/\kappa(\mathbf{D}_{II})$.

5.3.7 Relative Errors in the Group Velocity

In this section, the approaches for numerically calculating the group velocity, illustrated in Section 2.4, are compared. The relative errors in the group velocity for the *n*=1 mode are shown for frequencies around the cut-off frequency in Figure 5.20. Results for the 18 elements model are shown. A frequency increment of $\delta\Omega = 7.5 \cdot 10^{-3}$ $(\delta f = 1Hz)$ is chosen. The result from differentiation of the eigenvalue problem shows poor accuracy. This is because $\mathbf{D}_{LR}$ must be inverted which is ill-conditioned and the fact that the approach needs many matrix operations. Therefore numerical errors accumulate.

Although all relative errors become large near the cut-off frequency, both the power and energy relationship and the finite difference approaches show reasonable accuracy. Both the power and energy relationship and the finite difference method have advantages and disadvantages in terms of accuracy and calculation cost. When both the eigenvalues and eigenvectors are accurately calculated, the power and energy relationship seems an appropriate approach. However, the eigenvectors are likely to be less accurate than the eigenvalues such that the finite difference method is typically more accurate. However, the finite difference method needs a small frequency increment around cut-off frequencies and branch points because the wavenumbers may change rapidly.

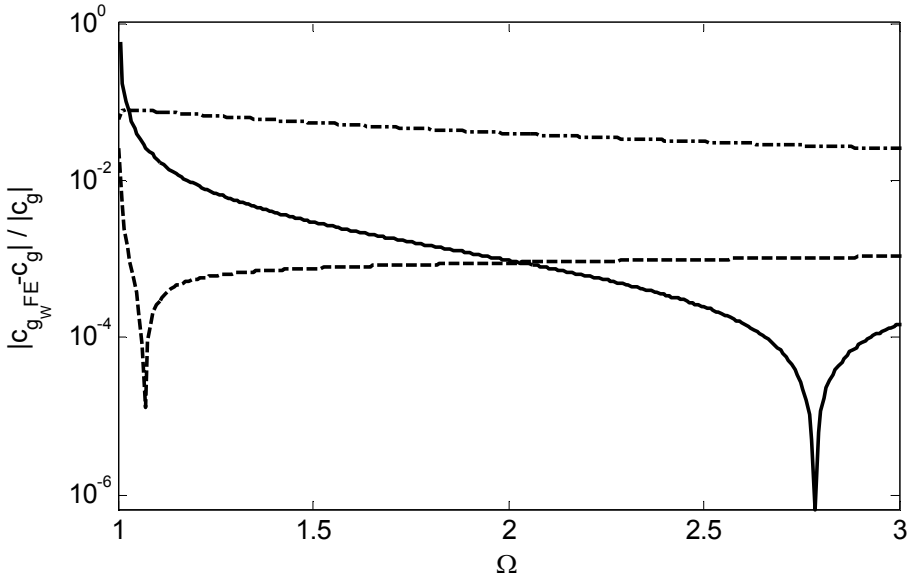

Figure 5.20: Relative errors in the group velocity: — finite difference, – – power and energy relationship, –·– differentiation of the eigenproblem.

6. CONCLUSIONS AND DISCUSSION

6.1 Concluding Remarks

In this report, the numerical issues for the waveguide finite element (WFE) method have been discussed. In the WFE method, the transfer matrix, hence the eigenvalue problem, can be formed from the elementary mass and stiffness matrix of a general structure. However because the transfer matrix might be ill-conditioned, the conditioning of the matrix is essential for general complex structures. To improve the matrix conditioning, Zhong's approach [30] has been applied and the validity has been investigated. To calculate the eigenvectors, an SVD approach has been proposed to improve numerical errors and the validity evaluated.

Potential numerical errors have been discussed and categorised into the FE discretisation errors, the round-off errors due to the inertia term and errors induced by ill-conditioning.

The relative errors in the eigenvalues and eigenvectors were explained by the FE discretisation error and the round-off error due to the inertia term for rod and beam problems. Ill-conditioning becomes prominent for plate problems as the matrix size increases. The relationship between the condition number and the shape of a FE element was investigated. The FE model, specifically the length of a section of a structure Δ, is important to determine numerical errors. The FE model with internal nodes was used to alleviate the trade-off among the potential numerical errors. The 1st order approximation for the condensation was derived, which showed best accuracy at low frequencies.

Three approaches for numerically calculating the group velocity have been introduced and the accuracy investigated. The power and energy relationship and the finite difference method seem appropriate approaches specifically for general structures.

References

1. L. Brillouin 1953 *Wave Propagation in Periodic Structures (Second edition)*. Dover.
2. D. J. Mead 1986 *Journal of Sound and Vibration* 104(1), 9-27. A New Method of Analysing Wave Propagation in Periodic Structures; Applications to Periodic Timoshenko Beams and Stiffened Plates.
3. D. J. Mead 1971 *Journal of Engineering for Industry* August, 783-792. Vibration Response and Wave Propagation in Periodic Structures.
4. D. J. Mead 1973 *Journal of Sound and Vibration* 27(2), 235-260. A General Theory of Harmonic Wave Propagation in Linear Periodic Systems with Multiple Coupling.
5. B. Aalami 1973 *Trans. of ASME, Journal of Applied Mechanics* December, 1067-1072. Waves in Prismatic Guides of Arbitrary Cross Section.
6. R. M. Orris, M. Petyt 1974 *Journal of Sound and Vibration* 33(2), 223-236. A Finite Element Study of Harmonic Wave Propagation in Periodic Structures.
7. R. M. Orris, M. Petyt 1975 *Journal of Sound and Vibration* 43(1), 1-8. Random Response of Periodic Structures by a Finite Element Technique.
8. A. Y. A. Abdel-Rahmen 1980 *Matrix Analysis of Wave Propagation in Periodic Systems.* Ph.D. thesis, ISVR, University of Southampton.
9. D. J. Thompson 1993 *Journal of Sound and Vibration* 161(3), 421-446. Wheel-Rail Noise Generation, Part3: Rail Vibration.
10. L. Gry 1996 *Journal of Sound and Vibration* 195(3), 477-505. Dynamic Modelling of Railway Track Based on Wave Propagation.
11. L. Gry, C. Gontier 1997 *Journal of Sound and Vibration* 199(4), 531-558. Dynamic Modelling of Railway Track: A Periodic Model Based on a Generalised Beam Formulation.
12. L. Houillon, M. N. Ichchou, L. Jezequel 2005 *Journal of Sound and Vibration* 281, 483-507. Wave Motion in Thin-Walled Structures.
13. D. Duhamel, B. R. Mace, M. J. Brennan 2003 *ISVR Technical Memorandum No:922*. Finite Element Analysis of the Vibrations of Waveguides and Periodic Structures.
14. B. R. Mace, D. Duhamel, M. J. Brennan, L. Hinke 2005 *Journal of Acoustical Society of America* 117(5), 2835-2843. Finite element prediction of wave motion in structural waveguides.
15. L. Hinke, B. R. Mace, M. J. Brennan 2004 *ISVR Technical Memorandum No:932*. Finite Element Analysis of Waveguides.
16. J. M. Mencik, M. N. Ichchou 2005 *European Journal of Mechanics, A/Solids* 24(5), 877-898. Multi-Mode Propagation and Diffusion in Structures through Finite Elements.
17. M. Maess, N. Wagner, L. Gaul *Journal of Sound and Vibration* to appear. Dispersion Curves of Fluid-Filled Elastic Pipes by Standard FE-Models and Eigenpath Analysis.
18. M. M. Ettouney, R. P. Daddazio, N. N. Abboud 1997 *Computers and Structures* 65(3), 423-432. Some Practical Applications of the Use of Scale Independent Elements for Dynamic Analysis of Vibrating Systems.

19. J. F. Doyle 1997 *Wave Propagation in Structures, Second edition*. Springer-Verlag.

20. B. R. Mace 1984 *Journal of Sound and Vibration* 97, 237-246. Wave Reflection and Transmission in Beams.

21. L. Cremer, M. Heckl, B. A. T. Petersson 2005 *Structure-Borne Sound (Third edition)*. Springer-Verlag.

22. S. Finnveden 2004 *Journal of Sound and Vibration* 273, 51-75. Evaluation of modal density and group velocity by a finite element method.

23. L. A. Pipes 1963 *Matrix Methods for Engineering*. Prentice-Hall Inc.

24. L. N. Trefethen, D. B. III 1997 *Numerical Linear Algebra*. Society for Industrial and Applied Mathematics.

25. G. H. Golub, C. F. V. Loan 1996 *Matrix Computations (Third edition)*. Johns Hopkins University Press.

26. T. Gudmundsson, C. Kenney, A. J. Laub 1997 *SIAM Journal on Matrix Analysis and Applications* 18(4), 868-886. Small-Sample Statistical Estimates for the Sensitivity of Eigenvalue Problems.

27. J. H. Wilkinson 1965 *The Algebraic Eigenvalue Problem*. Oxford University Press.

28. S. V. Huffel, V. Sima, A. Varga, S. Hammarling, F. Delebecque 2004 *IEEE Control System Magazine* February, 60-76. High-Performance Numerical Software for Control.

29. C. Moler (2004). *Chapter 10, Eigenvalues and Singular Values.* http://www.mathworks.com/moler/eigs.pdf, *avaiable* 19/12/2005.

30. W. X. Zhong, F. W. Williams 1995 *Journal of Sound and Vibration* 181(3), 485-501. On the Direct Solution of Wave Propagation for Repetitive Structures.

31. W. X. Zhong, G. Cheng 1991 *Proceedings of the Asia-Pacific Conference on Computational Mechanics*, Blakema, Rotterdam, 373-378. Regularization of Singular Control and Stiffness Shifting.

32. W. X. Zhong, F. W. Williams 1992 *Proceedings of the Institution of Mechanical Engineers, Part C* 206, 371-379. Wave Problems for Repetitive Structures and Symplectic Mathematics.

33. G. W. Stewart 1972 *SIAM Journal on Numerical Analysis* 9(4), 669-686. On the sensitivity of the Eigenvalue Problem $Ax=\lambda Bx$.

34. V. C. Klema, A. J. Laub 1980 *IEEE Transactions on Automatic Control* AC-25(2), 164-176. The Singular Value Decomposition: Its Computation and Some Applications.

35. M. Petyt 1990 *Introduction to Finite Element Vibration Analysis*. Cambridge University Press.

36. K. F. Graff 1975 *Wave Motion in Elastic Solids*. Dover.

37. J. R. Banerjee 2003 *Journal of Vibration and Acoustics, Trans. of ASME* 125, 351-358. Dynamic Stiffness Formulation and Its Application for a Combined Beam and a Two Degree-of-Freedom System.